A design method for timber grid shells

MSc thesis

Maarten Kuijvenhoven

February 2009

Delft
University of
Technology

A design method for timber grid shells

MSc thesis

Maarten Kuijvenhoven

Student ID: 1170244

Supervisors: Prof. Dr. Ir. J.G. Rots
TU Delft, section of Structural Mechanics

Dr. Ir. P.C.J. Hoogenboom
TU Delft, section of Structural Mechanics

Dr. Ir. J.W.G. van de Kuilen
TU Delft, section of Building and Structural Engineering

Ir. J.L. Coenders
TU Delft, section of Building and Structural Engineering
Structural Design Lab
Arup

Ir. M.H. Toussaint
DHV structural engineering, The Hague

TU Delft
Delft University of Technology

Preface

This thesis was written to conclude my education in Civil Engineering at Delft University of Technology.
I would like to thank my supervisors for their help and my family and friends for their support.
The data and scripts used in this thesis can be obtained from the author. E-mail address for correspondence: Maarten.Kuijvenhoven@gmail.com.

Maarten Kuijvenhoven

Delft, February 2009

Abstract

Timber grid shells are a special type of structures that combine structural efficiency with appealing looks. In addition, they have a very limited impact on natural resources when designed properly. They can also be built in a relatively short time by building it initially as a flat grid of straight members and then bend it into the desired shape.

Looking at the many advantageous properties of timber grid shells it could be expected that this kind of structure would be much more common. However, only a handful has been built so far. One explanation for this is that their relatively complex design process deters people from choosing for this type of structure.

In this thesis a new design method is proposed that makes use of a computer application that is developed specifically for the purpose of helping in the design of timber grid shells. It is investigated how such a design tool can be set up and what functionality it needs to have. To illustrate the concepts an actual design tool is developed in the C++ programming language based on a particle-spring approach. The design tool is able to find a feasible three-dimensional shape and corresponding system of forces of a grid shell based on any initial shape. Hereby limitations are taken into account that follows from the properties of timber such as maximum curvature due to bending.

The various components of the developed design tool are evaluated by comparing it with results obtained with other software and methods. It turned out that the results found by the design tool are satisfactory in general. It is concluded that there is a need for design tools in the design process of timber grid shells and that the proposed method can fulfil this very well.

Contents

1 Introduction

Shell structures are very efficient in spanning large distances with a minimum of material. Their load bearing efficiency results from the double curvature, which provides membrane action. This means that a distributed load on a thin shell will only lead to the development of normal and in-plane shear stresses. Bending stresses can generally be neglected and the stress field will be uniformly distributed over the cross section. These effects result in a very efficient structure. It should be noted that incompatible loading and support conditions often disturb pure shell action. In that case a combination of shell and bending theory needs to be applied (Hoefakker & Blaauwendraad, 2005).

Figure 1 Savill Garden grid shell

Grid shells differ from continuous shells by being built up of a collection of slender members instead of a continuous surface. These members are connected at their intersections to form a grid that lies on a double curved surface. This way shell behaviour is imitated (Toussiant, 2007). However, shear forces cannot be transmitted through the grid, so in order to create true shell behaviour some form of bracing has to be provided. This can be done by applying a continuous layer covering the grid (cladding) or by using diagonal bracing that triangulates the grid

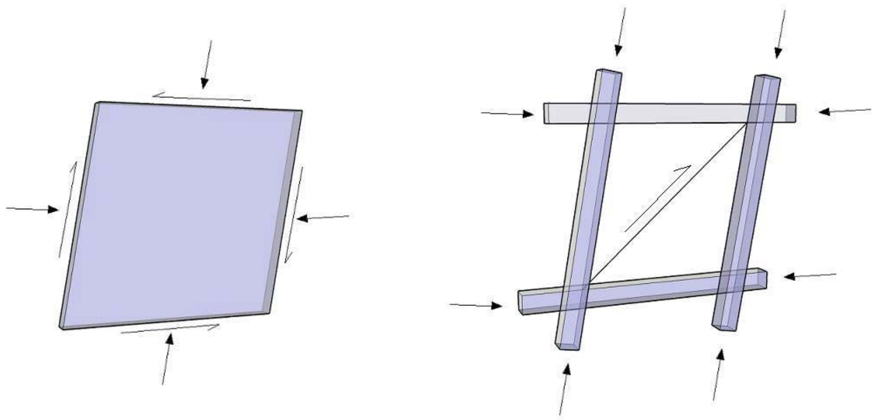

Figure 2 *Forces in continuous and grid shell elements*

When timber is used for the members of the grid shell, an interesting construction method can be used. Firstly, a flat grid is created, which makes it relatively easy to assemble all the laths and connect them together. Once the grid is completed it can be bent to the desired shape and fixed at its supports.

Figure 3 *Construction of the Weald and Downland grid shell*

Although this can be a very fast, and therefore economic, way of building a shell structure it has not been done very often.

Perhaps the most famous timber grid shell that was built this way is the Multihalle in Mannheim that was built for the Bundesgartenschau in 1975. Another more recent example is the Weald and Downland Gridshell built in 2002 for the open-air museum in Chichester. Although there are a few more examples of timber grid shells, only those in Mannheim, Chichester and Windsor were built by bending initially straight members into shape. The Savill Garden Grid shell in Windsor was built slightly different. Here a temporary formwork was built first, onto which the laths could be placed by bending them in a controlled manner. It seems like this made the time needed for construction much longer and the overall building cost much higher compared to simply bending it into shape without elaborate temporary formwork, but this decreased the amount of timber failures during construction[1].

One of the main problems with bending the grid into shape is that it is very difficult to accurately find the shape of the laths in the grid once the shell is standing on its own. This is necessary in order to build and clad the structure in practice. Another problem is the difficulty to predict the forces that will occur in the timber. This can lead to a large amount of failures of the timber during construction.
For the design of the Multihalle in Mannheim only very limited use could be made of computer technology, so for a large part the engineers had to resort to building physical models to find the shape.

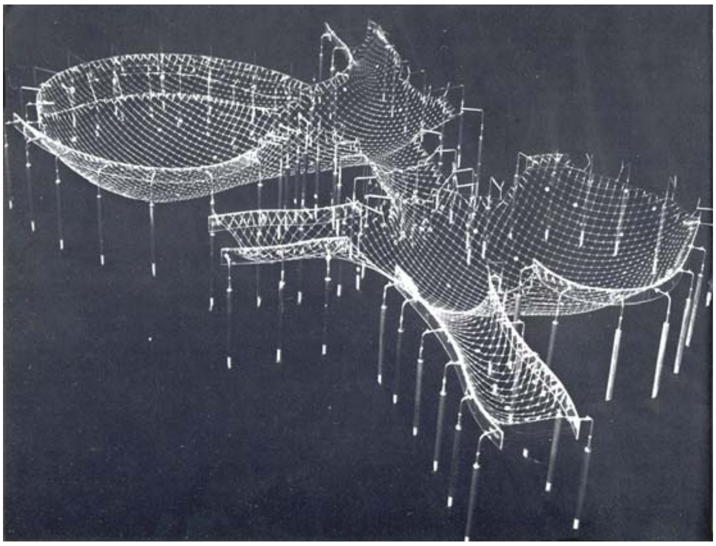

Figure 4 Hanging chain model of the Mannheim Multihalle

[1] For a more elaborate description of the properties and backgrounds of timber grid shells, see Toussaint, 2007

First a hanging chain model was created, which then had to be translated to the geometry of an actual grid that could be built in practice. This was done by determining the coordinates of the grid points of the model with stereo photography and creating additional models to investigate stability properties.

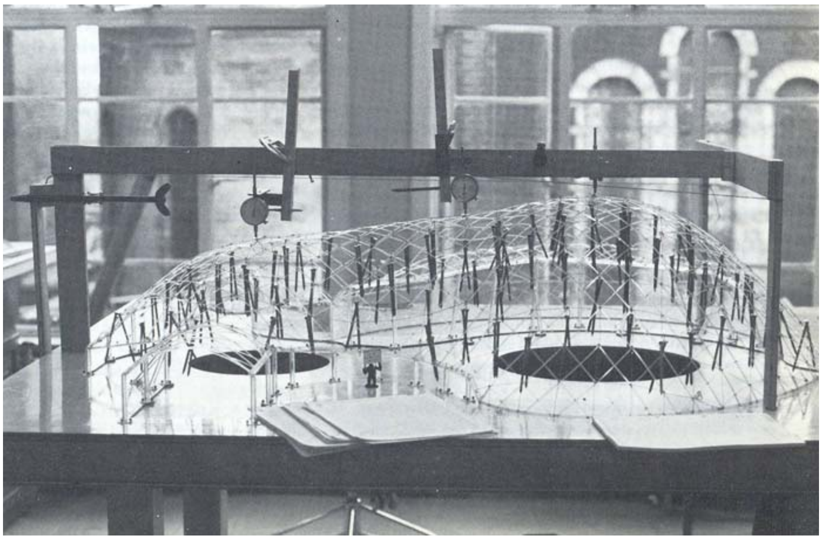

Figure 5 *Scale model used in the design of the Mannheim Multihalle*

Clearly, the significant improvements in computer technology since then can be used to make the design process much easier. The standard computers in use at every engineering firm today have much more computing power available than there was in the 1970's. However, standard structural engineering software does not exist for this purpose, so new computer applications have to be developed specifically for this.
In this thesis the possibilities of such design tools are investigated. The goal of the research can therefore be stated as:

To determine a feasible set-up for a design tool that can model the shape and internal forces of a timber grid shell

2 Design tools for timber grid shells

In this chapter it will be investigated what design tools, which can be used in the realisation of timber grid shells, should ideally consist of. A general approach for the development of such design tools will be described.

2.1. General requirements

In order to develop a useful design tool there are several requirements that have to be taken into account. The design tool has to fill in the gap between the aesthetic looks and functional requirements determined beforehand, and the shape of the grid shell that can actually be built.

The tool should be easy to use and give insight in the process so that architect and engineer can work together to find the best possible shape that is functional and makes efficient use of material at the same time.

For the full structural analysis of the final geometry use be made of other software. The format of the output of the design tool should therefore be in line with input for commonly used structural analysis software.

Finally, It should preferably be accessible in the sense that it is not dependent of advanced software that is expensive and takes a lot of skill to use.

2.2. Possible functionality

The most important purposes of the design tool are to define the geometry as it can actually be build and to predict the forces that will be present in the grid shell during construction. For timber grid shells, unlike most other structures, the construction phase is the most critical stage of its life. Since the shape is closely linked to the forces that are present in the timber and the support reactions, these must always also be known when the final geometry is known.

The following can be included in the output to be produced by the design tool, or at least an indication should be given:

- Geometry of the final shape
- Internal forces
- Support reactions
- Forces needed to bend the grid into shape
- Geometry of the grid before it is bend into shape
- Information on the accuracy of the results

2.3. Proposed set-up

At the most basic level the design tool should consist of three components:

- Material model
- Approximation of the target shape
- Equilibrium form finding procedure

Ideally the approximation of the target shape and the equilibrium form finding are performed simultaneously such that the shape that best approximates the target shape given the set of criteria specified beforehand is also the geometry that the timber grid shell will have when built. However, this is very hard to accomplish because the exact final shape depends only on the location of the supports and the length of the laths, so any further restrictions on the shape cannot be applied anymore.

A solution is to separate the form finding procedure into two stages. First the target shape is approximated as good as possible and subsequently the equilibrium shape is found that corresponds to the grid shell standing on its own. The cost of this is a difference in the two shapes, which is hopefully only marginal. This is also what can be observed in practice, after the grid is bent into shape and the internal supports used for erection are being removed. This has a direct effect on the shape of the grid shell, which must change slightly due to the different support conditions.

2.3.1. Material model

The behaviour of the timber has to be modelled in some way such that the computer is capable of working with it. Discretisation is therefore needed. A possible approach is to model the material by a system of springs that are connected together in particles that represent the geometry of the timber. The relations that represent the material behaviour is modelled in the springs. This system is widely know as the discrete element method in structural mechanics and is used for example in the development of the structural analysis programme Tilly (Welleman, 1992). Large deformations are very commonly modelled in this way in the field of computer graphics for cloth simulation. Axel Killian and John Ochsendorf have described how these large deformation models of particle spring systems can be used in the form finding of shell structures. However, they only considered the axial forces. For the modelling of timber grid shells this is not sufficient especially since bending is very important in this case. Therefore a description of how the concept can be extended will be given. Within a structural element the following actions can occur:

- Tension
- Compression

- Bending
- Shear
- Torsion

Each of these actions can be represented by a relation that defines a certain internal force acting on the particles (or system of forces) for every position of two or more particles relative to each other. For instance the tension and compression actions can be modelled by:

$$\overline{F} = - k \times \overline{u}$$

Where *k* is a stiffness parameter or function and *u* is the difference of the distance between the two particles and a certain reference distance. Graphically this can be represented as a spring. Similarly the bending action can be modelled by rotational springs with the relation;

$$\overline{M} = k \times \theta$$

With these two types of springs the overall behaviour of a simply supported beam could be modelled as depicted in Figure 6. The other two actions, torsion and shear can be modelled in the same manner but are more difficult to represent graphically.

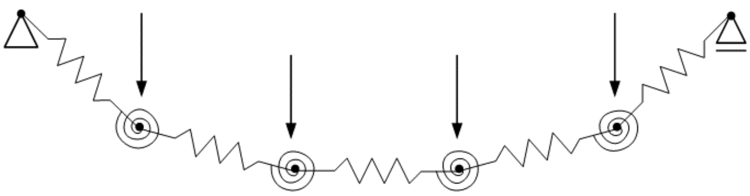

Figure 6 Discretisation of particles and springs

The degree of deformation of the grid can in general be deducted from the locations of the particles. For instance the angle that the two lines connecting one particle makes with its neighbours can be a measure for the degree of curvature at a certain section of the lath (see Figure 7). Likewise the (change in) distance between two particles can be a measure for the elongation. The same holds for shear and torsion effects as well.

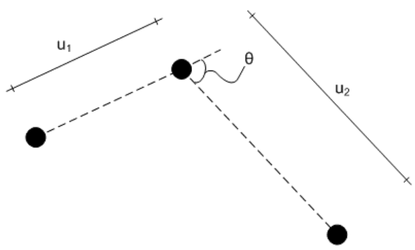

Figure 7 Calculation of rotation and distance based on coordinates of three grid points

The structural behaviour, and therefore indirectly the shape, is controlled by the forces acting on it. The supports are modelled by setting the resultant force to zero at those particles. Also the moment due to bending should be converted to a set of point loads in order to incorporate it into the model.

It can generally be assumed that the grid can be modelled by considering the connections between the laths (the grid points) as the particles. In general, use can also be made of intermediate additional particles, but for reasonable dimensions of the grid shell with lath spacing of about 0.5m to 1.0m the grid point density can be expected to accurately model the overall grid behaviour.

2.3.2. Shape approximation

Deforming a grid into a shell shape introduces stresses in the timber. When these stresses become too large the material will fail. It is very difficult to determine a shape for a timber grid shell where stresses remain within limits. For instance, in order to limit stresses due to bending, the curvature in the members should not be too large which provides an upper constraint to the deformation. However, in order to create an effective shell that is not too vulnerable to buckling a certain maximum span to height ratio is required, which gives a lower constraint to the bending of the laths. The laths should therefore be bent as much as possible. Since there is such a small range of possible geometries and the internal force distribution cannot easily be known, it cannot be expected that the first shape that is specified by the architect satisfies these demands, so a process is needed that approximates this target shape as good as possible.

Furthermore, the determination of any regular grid on a complex doubly curved surface is a task that in most cases cannot be accomplished without the help of a design tool such as those described in (Toussaint, 2007) and (Leuppi, 2002). Therefore, apart from the need to be able to define the final shape in which the grid is in equilibrium and that can ultimately be build, there is a need to come up with a suitable start-off shape. The design tool should be capable of doing this as well. It is hereby very important to clearly specify the criteria to which the geometry of the grid shell must conform. At least the following criteria have to be considered:

- (Combinations of) stresses sufficiently small
- Functional requirements of the internal space
- Maximum span to height ratio of the shell to prevent buckling
- Regular grid point spacing

If it is assumed that the functional requirements are satisfied in the target shape and have a bit of room for adjustments, it can be assumed that a shape that is as close as possible to this target shape still satisfies the functional requirements. The timber properties and dimensions of the laths indirectly specify a minimum span to height ratio of the shell since for smaller span to height ratios the laths will have to be bent further causing stresses to exceed the timber strength. It can be assumed that bending the laths as far as possible will provide a shape that is least likely to be vulnerable to buckling. This should still be checked with other existing software applied to the final geometry produced by the design tool. The first three criteria are therefore met if the target shape is approximated as closely as possible without exceeding limits on the stresses for wich failures occur.

To evaluate the stresses in the timber, use can be made of the checks that have to be satisfied according to the standards. For instance Eurocode 5 (EN-NEN 1995-1-1) gives a set of unity checks. If the design tool uses these checks as a criteria for the stresses, the chance of failures during construction and thereafter can be expected to be sufficiently small. Some of the checks from the Eurocodes that can be implemented are:

Tension parallel to the grain

$$\sigma_{t,0,d} \leq f_{t,0,d}$$

Combined bending and axial compression

$$\left(\frac{\sigma_{c,0,d}}{f_{c,0,d}}\right)^2 + k_m \frac{\sigma_{m,y,d}}{f_{m,y,d}} + \frac{\sigma_{m,z,d}}{f_{m,z,d}} \leq 1$$

$$\left(\frac{\sigma_{c,0,d}}{f_{c,0,d}}\right)^2 + \frac{\sigma_{m,y,d}}{f_{m,y,d}} + k_m \frac{\sigma_{m,z,d}}{f_{m,z,d}} \leq 1$$

Shear

$$\tau_d \leq f_{v,d}$$

Torsion

$$\tau_{tor,d} \leq k_{shape} \times f_{v,d}$$

The design tool should not only check the stresses, it should also alter the shape in case stresses are too large. In order to achieve this, a method is proposed in line with the particle spring system of the material model and the construction process as well. The general idea is to model the process of deforming a grid of initially straight laths towards the target shape and continuously measure the (combinations of) stresses while doing so. Forces are applied to the grid points generated by virtual springs connected between the laths and the target shape.

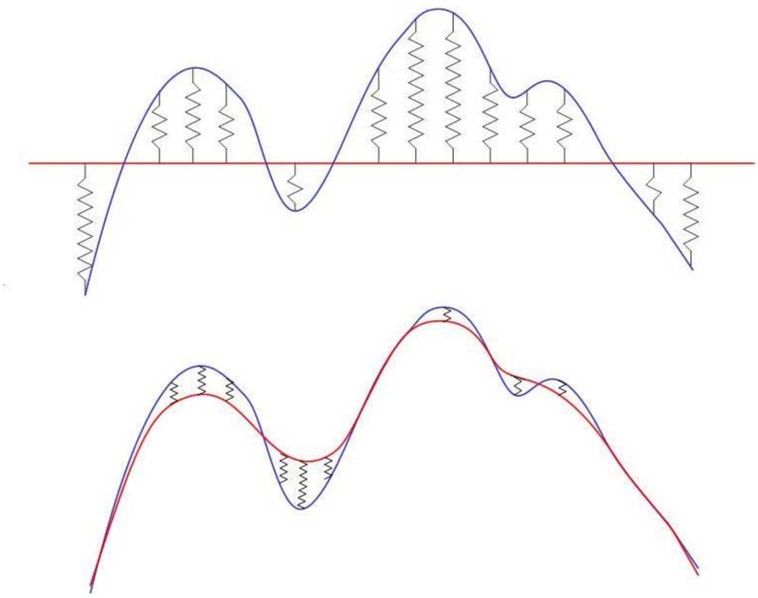

Figure 8 Shape approximation by springs

If the stress capacity is exceeded at a certain point in the grid at a given moment, the force deforming the grid towards the target shape has to be altered at this location such that the stress decreases. Ideally the shape will be altered such that only that type of stress that is too large (e.g. due to bending, torsion, compression etc.) is reduced. In the case of bending this could be implemented quite simply by reducing the relevant component of the force exerted by the shape spring on the lath, resulting in a smaller deviation from the initial straight member and therefore a reduction of the bending at that grid point. For the other actions like torsion it is slightly less straightforward, because the locations of the grid points surrounding the grid point where the torsion capacity is exceeded have to be altered in addition to the grid point itself.

2.3.3. Equilibrium form finding

After the shape approximation has finished, the resulting form is in equilibrium with the shaping forces. However, in practice these forces cannot be applied to the real structure after the construction phase. During construction external forces are applied to deform the grid, but thereafter the grid shell is supposed to be standing on its own where the deformed shape is maintained only by restricting movement at the supports. To find this final shape, the design tool has to let the deformed gird find its equilibrium shape with no external actions applied to it except for the restricted movement of the supports. The difference between the shape of the grid shell after shape approximation and the final shape found after equilibrium form finding should of course be as small as possible, because it is otherwise not known anymore if the final shape conforms to all the criteria stated before. The initial shape as specified by the architect (or engineer in the role of architect) should therefore be as realistic as possible. The more realistic, the smaller the difference between the two shapes can be expected to be.

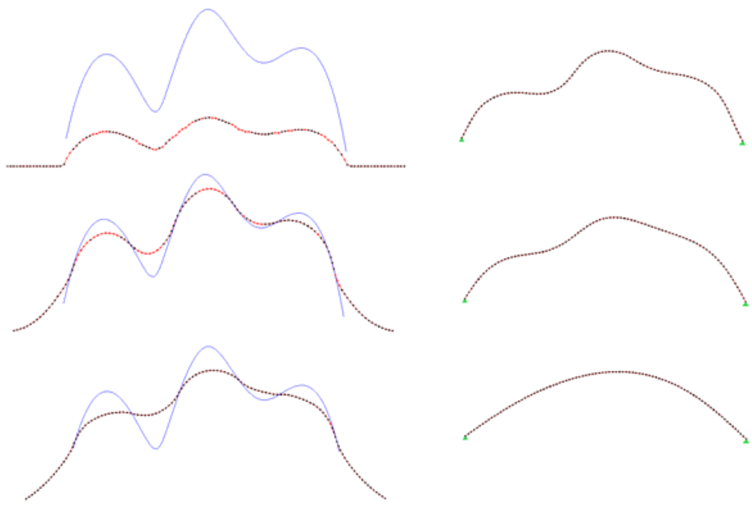

Figure 9 *Entire form finding procedure for a line element*

2.4. Dynamic relaxation

So far the set-up of the design tool described considers the grid shell to be modelled discretely into the grid points (at the connections between laths) and applying forces to them that can be due to either internal or external actions. A method is needed that can work with these principles to find a shape for the grid shell that is in equilibrium.

There are several methods available to do this, as described in (Toussaint, 2007) the most relevant one being the dynamic relaxation method as described in (Barnes, 1999). Here the resultant of all the forces working on a grid point is thought to accelerate the grid point in the direction of the resultant of the forces. According to Newton's second law of motion, the acceleration is found by dividing the force by the mass *m* of the particle, which can be a virtual mass and does not have to correspond to the actual mass of the grid points in the timber grid shell, because it is only used for the form finding process.

$$\bar{a} = \frac{\bar{F}}{m}$$

If this acceleration is integrated for a certain time step a velocity is found. If this velocity is integrated again over a certain time step a distance is found that the grid point can be thought to have moved in the time step under consideration. This has to be done for all the grid points, which will result in a new geometry of the grid shell. In this new geometry the internal forces will have changed and the procedure is repeated. This is done many times, constantly changing the geometry of the grid shell. The grid points will always move in the direction of a location where they are in equilibrium. If all the grid points have arrived at a position where they are in equilibrium the geometry of the grid will not change anymore, because all the force resultants are now zero. Therefore the equilibrium shape of the overall grid shell is found. In order to prevent the grid from oscillating about the equilibrium shape, damping has to be applied. That way the dynamic equilibrium will turn into static equilibrium. This damping can consist of viscous damping where the grid points are slowed down by a certain drag force relative to their velocity. Another (more common) method is to measure whether a peak in the total kinetic energy of the system occurs. When a peak is detected all velocities are set to zero. The peaks in kinematic energy will decrease each time until finding equilibrium. This method is known as the dynamic relaxation with kinematic damping method.

In the suggested set-up of the design tool, this method is used twice to find an equilibrium shape. Firstly during the shape approximation stage and thereafter to find the final shape of the grid shell as it can stand on its own in practice.

The integration of the acceleration and velocity of the grid points has to be done numerically. Standard ways of doing so are the Euler method, the Trapezium method and the fourth order Runge Kutta method (lecture notes WI3097). These can be either implicit or explicit. Implicit methods are more suitable in this case, because the high stiffness of the spring elements will otherwise lead to numerical instability (Killian & Ochsendorf). The implicit fourth order Runge Kutta method is not the fastest method but is commonly used because of its good convergence properties. The integration scheme for this method is as follows:

$$
\begin{array}{l|l}
k_1 = \bar{a} & k_1 = \bar{v} \\
k_2 = \bar{a} + h \times \frac{k_1}{2} & k_2 = \bar{v} + h \times \frac{k_1}{2} \\
k_3 = \bar{a} + h \times \frac{k_2}{2} & k_3 = \bar{v} + h \times \frac{k_2}{2} \\
k_4 = \bar{a} + h \times k_3 & k_4 = \bar{v} + h \times k_3 \\
\bar{v} = \bar{v} + \frac{h}{6} \times \left(k_1 + 2 \times k_2 + 2 \times k_3 + k_4\right) & \bar{u} = \bar{u} + \frac{h}{6} \times \left(k_1 + 2 \times k_2 + 2 \times k_3 + k_4\right)
\end{array}
$$

Here a, v and u are the acceleration, velocity and distance travelled respectively. The parameter h denotes the step size, this should be sufficiently small to ensure numerical stability. However, a step size that is chosen too small will result in a very slow integration process.

3 The development of a design tool

To illustrate the proposed methods described in the previous chapter a design tool has been developed in the C++ programming language.

3.1. General approach

The method used is based on a particle spring system built-up of both translational and rotational springs, the differential equation following from this is solved using a fourth order Runge-Kutta method. Torsion and shear effects are not taken into account. The tool will iterate until finding equilibrium of forces in all grid points. Subsequently, a dxf file is created which can be imported into other existing software for further analysis. This works by creating a grid of line elements in two perpendicular directions. This grid is then deformed towards the desired input shape, making the members subject to bending about both the principal axis of their cross section. For the derivation of the formulas differentiation is necessary between the global xyz coordinate system and the local coordinate systems of the beams.
The members are laid out in a grid with two sets of members that are initially perpendicular. The first direction is called i and the other j. When the calculation starts these directions are equal to the x- and y-directions, but when the grid starts to deform this is generally no longer the case. The directions of i and j change with every grid point.

The script has been divided into several smaller files instead of having one big file containing all of the programming language. This makes it easier for others to understand how the programme is working, where to find a specific part of the script and to make additions to it at a later stage. As described in the previous chapter, the design tool is set up to work in two separate stages. In Figure 10 the flow chart of the first stage is shown. During this stage an equidistant grid is created approximating the surface of the target shape. The design tool will checks each grid point for capacity to resist stresses due to double bending. If the stress capacity is exceeded somewhere the shape is altered indirectly through the shape forces in order to reduce the stress at that point.

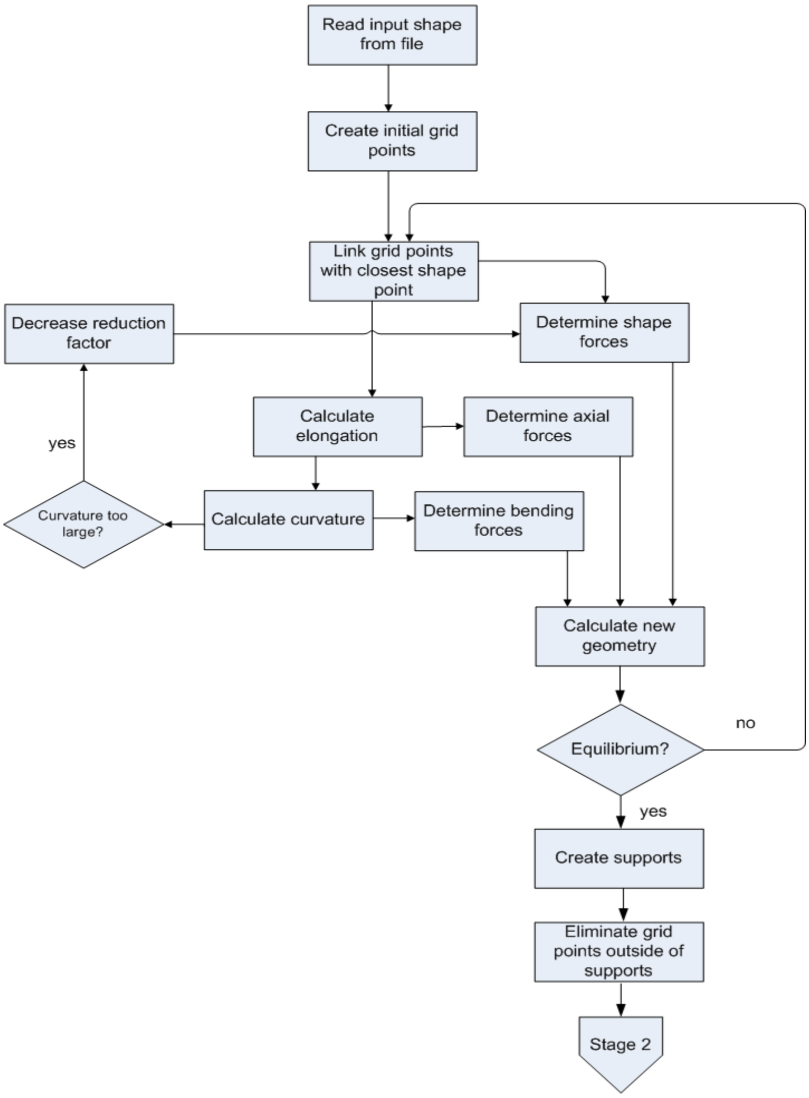

Figure 10 *Flow chart first stage*

The output of the first stage acts as input for the second stage. In the second stage the equilibrium shape is sought that would appear if the grid shell would stand on its own. In Figure 11 the flow chart for the second stage is shown. This is a more basic version of the script of the first stage. The shape forces are now no longer present, but instead external forces can be applied. At the end the geometry of the grid is documented as a dxf file together with a report that supplies additional information.

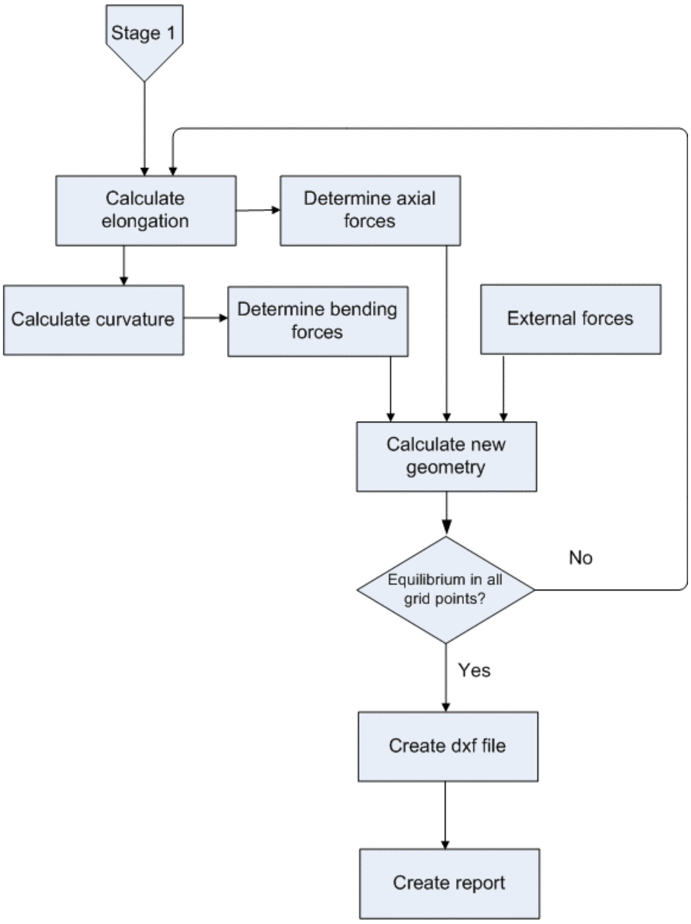

Figure 11 *Flow chart second stage*

The switch to the second stage comprises mainly of a change of boundary conditions. In the first stage the beam is supported by the shape approximating springs, in the second stage these springs are no longer active and the beam is supported by hinges at either end instead. The constraints corresponding to the hinged supports are placed at the grid points that lie closest to the edge of the target shape. All grid points that lie outside the two support grid points are eliminated.

3.1.1. Input

The input variables and target shape can be specified in txt files that have to be saved in the same folder as the executable is in.

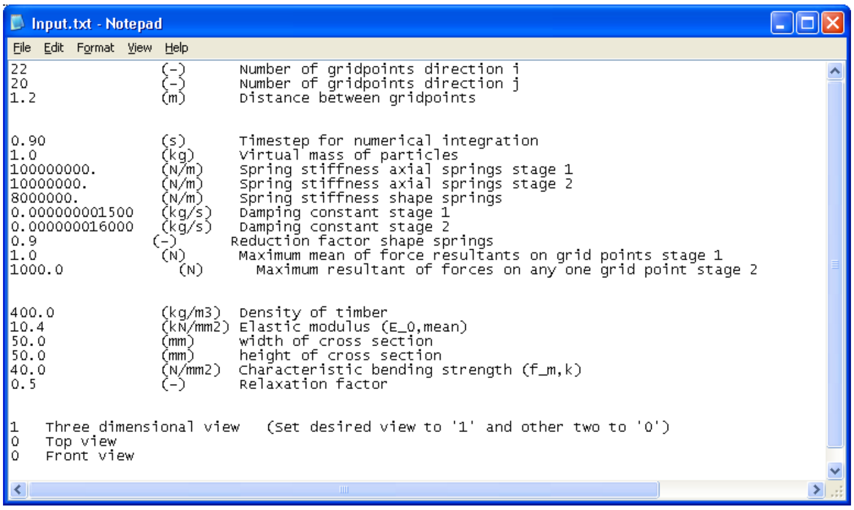

Input.txt - Notepad

File Edit Format View Help

```
22                (-)      Number of gridpoints direction i
20                (-)      Number of gridpoints direction j
1.2               (m)      Distance between gridpoints

0.90              (s)      Timestep for numerical integration
1.0               (kg)     Virtual mass of particles
100000000.        (N/m)    Spring stiffness axial springs stage 1
10000000.         (N/m)    Spring stiffness axial springs stage 2
8000000.          (N/m)    Spring stiffness shape springs
0.000000001500    (kg/s)   Damping constant stage 1
0.000000016000    (kg/s)   Damping constant stage 2
0.9              (-)      Reduction factor shape springs
1.0               (N)      Maximum mean of force resultants on grid points stage 1
1000.0              (N)      Maximum resultant of forces on any one grid point stage 2

400.0             (kg/m3)  Density of timber
10.4              (kN/mm2) Elastic modulus (E_0,mean)
50.0              (mm)     Width of cross section
50.0              (mm)     Height of cross section
40.0              (N/mm2)  Characteristic bending strength (f_m,k)
0.5               (-)      Relaxation factor

1   Three dimensional view   (Set desired view to '1' and other two to '0')
0   Top view
0   Front view
```

Figure 12 *Input variables*

The input variables are divided into four groups. With the first three the size and dimensions of the grid can be specified. With he next ten variables the numerical stability of the calculation procedure can be controlled. Also the equilibrium can be specified for which the design tool will consider the grid shell to have converged. The properties of the timber laths can be specified with the next six variables. Finally way the development of the grid is visualised can be indicated.

The geometry of the target shape should be given as a set of coordinates of points that lie on the target shape’s surface. The design tool can handle up to one million specified points. Using software such as Rhinoceros it is fairly easy to make such a file for any given shape.

3.1.2. Output

Output is given the form of a dxf file containing all the coordinates of the final grid and a txt file containing additional information. The dxf file can be opened in other structural analysis software for further analysis of the grid shell. The txt file contains information on:

- Accuracy of the calculation
- Shape forces needed to deform the grid
- Support reactions
- Exceeded stresses
- Remaining bending moments after relaxation

3.2. Internal forces

For accurate modelling of the structural behaviour of the timber laths formulas have to be derived to model the flexural and axial rigidity.

3.2.1. Compression and tension

The forces following from the translational springs can be either compression or tension forces.

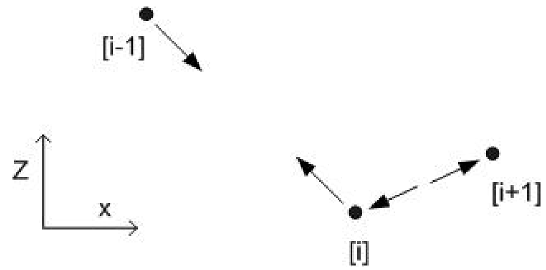

Figure 13 *Axial spring forces*

The equilibrium length of the springs is determined beforehand from the initial geometry of the beam. If the distance between two grid points in a certain configuration is different than this equilibrium length a force is applied to these grid points calculated from

$$F = -k \times u$$

Here *u* is the difference between the current distance and the equilibrium length (negative when the distance is smaller than the equilibrium length), and *k* is the spring stiffness. For this spring stiffness a non-linear relation is used because the high axial stiffness of the timber would otherwise make the script very vulnerable to numerical instability. By using a non-linear relation as depicted in Figure 14 the stability behaviour is much better while still ensuring equal distances between grid points. Since the stiffness is not based on realistic timber properties, the resulting forces are virtual and cannot be used for analysis of the internal stresses, but only to keep the grid points at a fixed distance from each other. It is assumed that bending is the main action that will cause failure of the timber laths so axial forces can be neglected in the stress check without losing much accuracy.

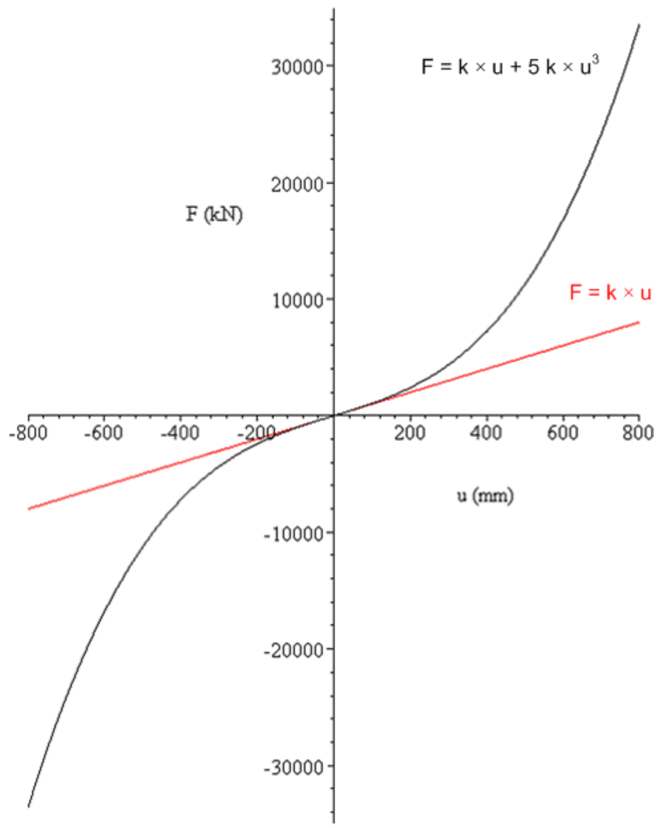

Figure 14 *Non-linear spring stiffness*

The forces have an x-, y- and a z-component and are applied either negatively or positively corresponding to the depicted coordinate system.

3.2.2. Bending

Bending behaviour is slightly more complicated. Below the derivation of the formulas for the two-dimensional case is given. For three dimensions the double bending behaviour makes things more difficult but the same method can be applied.

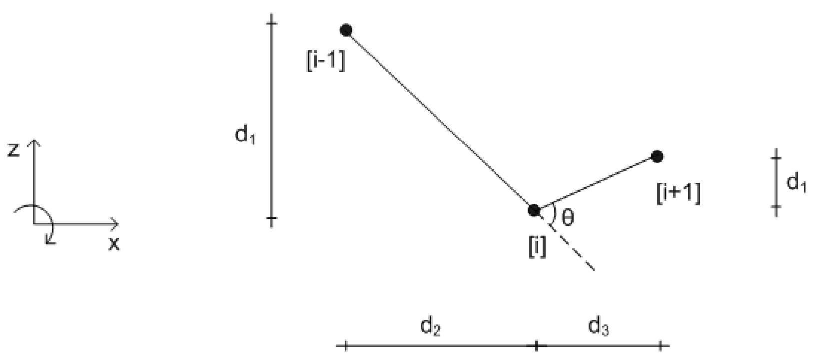

Figure 15 *Three subsequent grid points in two-dimensional space*

The four distances are defined to be positive when the respective x- and z-coordinates of subsequent grid points increase. In the figure above d_1 would therefore be negative and all other distances positive.

The angle θ is calculated from:

$$\theta = \arctan\left(\frac{d_1}{d_2}\right) - \arctan\left(\frac{d_4}{d_3}\right)$$

The moment due to this rotation is:

$$M = \theta \times k_{rot}$$

Where k_{rot} is the rotational spring stiffness found from:

$$k_{rot} = \frac{EI}{\Delta L}$$

Where ΔL is the length between subsequent grid points and EI is the pre-specified flexural rigidity. The derivation for this expression is as follows:

$$\left.\begin{array}{l} M = EI \times \kappa \\ M = k_{rot} \times \theta \\ \theta = \Delta L \times \kappa \end{array}\right\} \rightarrow \quad k_{rot} \times \Delta L \times \kappa = EI \times \kappa \quad \rightarrow \quad k_{rot} = \frac{EI}{\Delta L}$$

The moment M is converted to equivalent point loads acting on the three grid points under consideration.

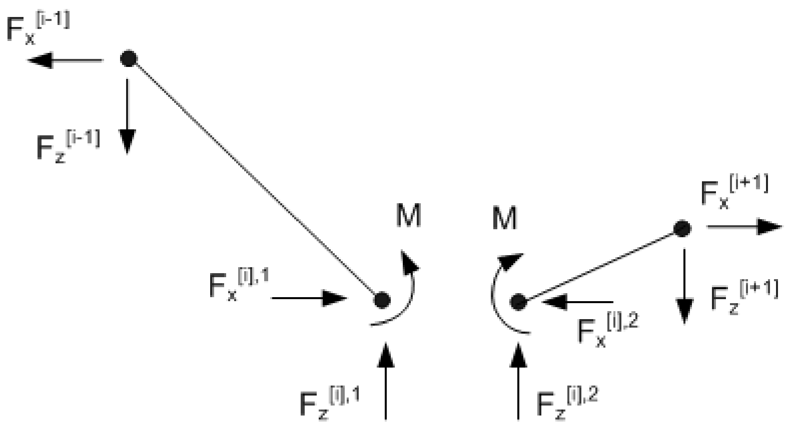

Figure 16 Bending forces

If d_1 is negative and d_4 is positive (as is the case in Figure 16), the forces can be found as:

$$F_x^{[i-1]} = \frac{M}{d_1 + \frac{d_2^{\,2}}{d_1}}$$

$$F_z^{[i-1]} = \frac{M}{d_2 + \frac{d_1^2}{d_2}}$$

$$F_x^{[i+1]} = \frac{-M}{d_4 + \frac{d_3^2}{d_4}}$$

$$F_z^{[i+1]} = \frac{M}{d_3 + \frac{d_4^2}{d_3}}$$

$$F_x^{[i]} = -F_x^{[i-1]} - F_x^{[i+1]}$$

$$F_z^{[i]} = -F_z^{[i-1]} - F_z^{[i+1]}$$

This procedure is repeated for every grid point, with the forces on every grid point due to bending in the next- and previous grid point being added to the forces due to bending in the grid point itself.

3.2.3. Calculation of the new geometry

The internal forces from bending and tension/compression are added together with any externally applied loads for every grid point to find the force resultants. For the numerical integration use is made of a fourth order Runge-Kutta method. The following expressions are used to obtain the new x-coordinate of a grid point (to find the new y- and z-coordinates similar expressions are used):

$$a_x = \frac{F_x}{m}$$

$$\begin{aligned} k_1 &= a_x \\ k_2 &= a_x + h \times \frac{k_1}{2} \\ k_3 &= a_x + h \times \frac{k_2}{2} \\ k_4 &= a_x + h \times k_3 \\ v_x &= c \times \left(v_x + \frac{h}{6} \times \left(k_1 + 2 \times k_2 + 2 \times k_3 + k_4 \right) \right) \end{aligned}$$

$$\begin{aligned} k_1 &= v_x \\ k_2 &= v_x + h \times \frac{k_1}{2} \\ k_3 &= v_x + h \times \frac{k_2}{2} \\ k_4 &= v_x + h \times k_3 \\ x &= x + \frac{h}{6} \times \left(k_1 + 2 \times k_2 + 2 \times k_3 + k_4 \right) \end{aligned}$$

When every grid point has been assigned a new x-, y- and z-coordinate the whole procedure is repeated with the new geometry. The factor *c* in the expression for the velocity of the particles is the damping constant which ensures the movement of the structure will reduce with every iteration, which prevents the structure from vibrating indefinitely. The iteration process will stop when the resultant of the forces on each grid point is sufficiently small, that is, the forces on all grid points are in equilibrium.

This is implemented by taking the sum of all forces in both directions on all grid points and to demand this to be sufficiently small (for example less than 0,1 N).

3.3. Shape approximation

The beam model (the red line in the figure below) is considered to be attached to the target shape (the blue line) by strong tension springs connected to the grid points. These springs will deform the beam such as to approach the desired target shape.

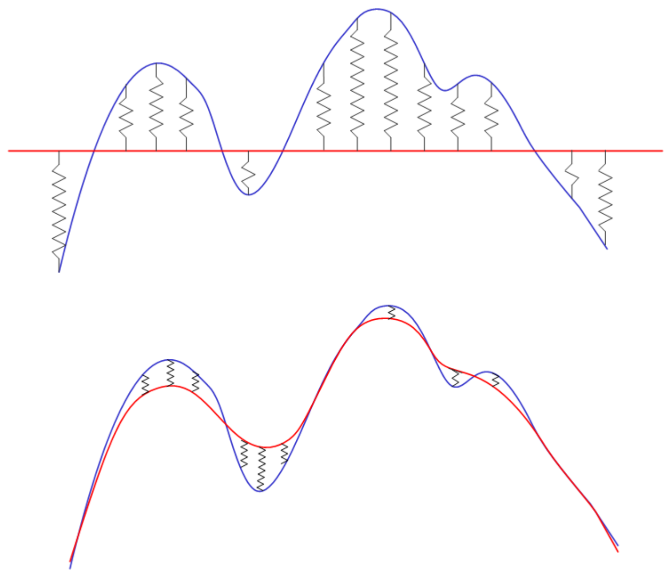

Figure 17 Shape approximation springs

As was described in the previous chapter, the curvature of the beam can be checked by looking at the position of the grid points relative to their neighbouring grid points. If this curvature is larger than a certain value specified beforehand, the stiffness of the spring connecting the beam and the input shape is reduced at that point. This will allow the beam to move away from the input shape at that point and thereby reducing the curvature. In the design tool the shape approximation springs have no horizontal components, so the grid is only vertically pulled towards the target shape. Better would be to have the direction of the springs to be normal to the target shape surface, but this makes the script much more complicated.

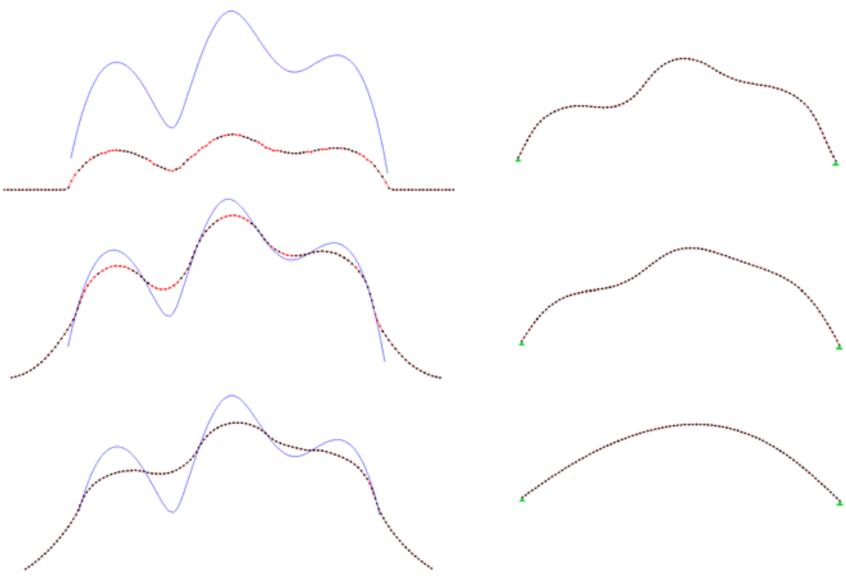

Figure 18 Form finding

The form finding procedure continues after the shape approximation by finding the shape of the laths they will take on if they are only supported at their end points. This is shown on the right of Figure 18. For the two-dimensional case this will always be a parabolic like shape, but in three dimensions this does not have to be the case because the laths will restrain each other.

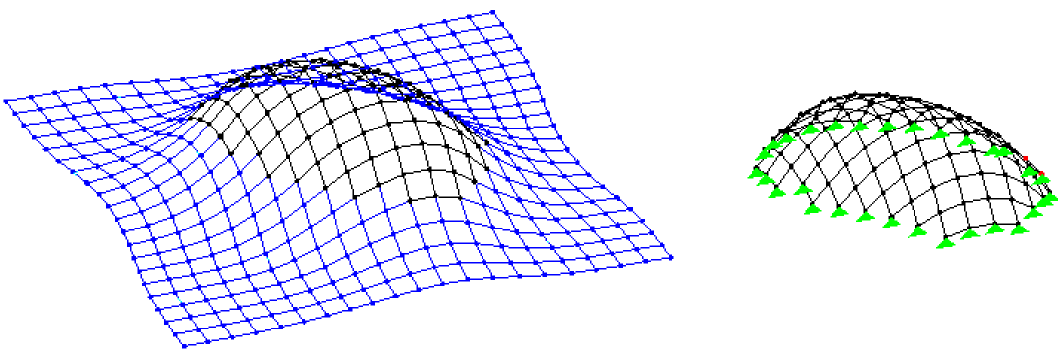

Figure 19 Shape approximation of a three dimensional surface

3.4. Stress analysis

The design tool checks if the stress due to bending does not exceed the maximum allowable stress immediately after construction as indicated in the Eurocodes. If this stress is found to be too large, the shape is altered such that the stresses decrease at that point. Four variables have to be specified by the user of the design tool:

$E_{0,mean}$	mean value of modulus of elasticity
$f_{m,k}$	characteristic bending strength

b width of the cross section

h height of the cross section

It is assumed that only rectangular cross sections are used.

3.4.1. Determination of design bending stress

The stress in a member at a certain grid point is calculated from the angle between a series of three subsequent grid points.

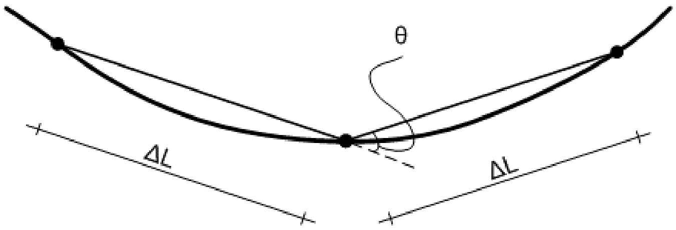

Figure 20 Determination of rotation in members

In three-dimensional space a distinction is made between in-plane rotations (θ_z) and out-of-plane rotations (θ_{xy}).

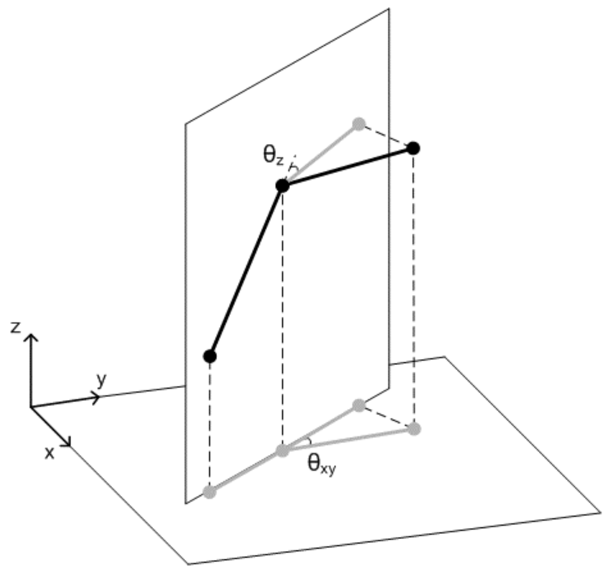

Figure 21 Determination of rotations between subsequent grid points

The rotations in the members are found from the grid point coordinates. The moments due to these rotations are:

$$M_{d,xy}=\theta_{xy}\times k_{rot}$$

$$M_{d,z}=\theta_{z}\times k_{rot}$$

Where k_{rot} is the rotational spring stiffness found from lumping the flexural rigidity of the lath into the grid points:

$$\left.\begin{array}{l} M = E_d \times I \times \kappa \\ M = k_{rot} \times \theta \\ \theta = \Delta L \times \kappa \end{array}\right\} \rightarrow k_{rot} \times \Delta L \times \kappa = E_d \times I \times \kappa \rightarrow k_{rot} = \frac{E_d \times I}{\Delta L}$$

Where:

$$E_d = \frac{E_{0,mean}}{\gamma_M} = \frac{E_{0,mean}}{1.3}$$

$$I_{zz} = \frac{b \times h^3}{12}$$

$$I_{yy} = \frac{h \times b^3}{12}$$

For the calculation of the second moment of area the cross section as depicted in Figure 22 is assumed for the laths.

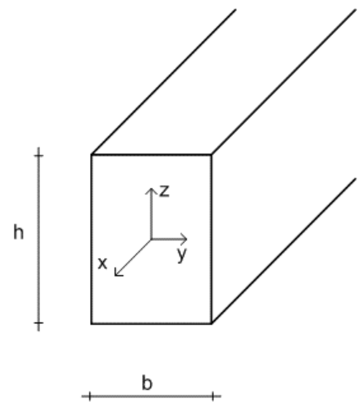

Figure 22 Cross section

The design bending stresses can now be obtained from:

$$\sigma_{m,z,d} = \frac{M_{d,z} \times \left(\frac{1}{2} h\right)}{I_{zz}}$$

$$\sigma_{m,y,d} = \frac{M_{d,xy} \times \left(\frac{1}{2} b\right)}{I_{yy}}$$

In the developed design tool it is assumed that the orientation of the cross section does not change with its position along the member. In other words, the z-axis of the local coordinate system of Figure 22 always has an equal orientation as the z-axis of the global coordinate system.

3.4.2. Determination of design bending strength

The capacity of the cross section to resist bending stress is checked according to section 6.1.6 of EN 1995-1-1.

The design bending strength is found from:

$$f_{m,z,d} = k_{mod} \frac{f_{m,k}}{\gamma_M} \times k_h$$

Where:

$$k_h = \min \begin{cases} \left(\frac{150}{h}\right)^{0.2} \\ 1.3 \end{cases}$$

$$k_{mod} = 0.9$$

$$\gamma_M = 1.3$$

Technically the factors k_{mod} and γ_M are not required since the construction stage is being considered and they only need to be applied for the checks on the completed building. However, they are still included in order to ensure some reserve strength to make up for otherwise disregarded torsion and shear effects. For most (rectangular) cross sections the design bending strenght amounts to:

$$f_{m,z,d} \cong 0.9 \times f_{m,k}$$

This is considered to be an acceptable factor to ensure sufficient capacity in the case of combined torsion and double bending, especially since the maximum stress due to torsion is never at the same location in the cross section as the maximum stress due to double bending (see Figure 23). Maximum stress due to double bending will always be somewhere at one of the corners of the cross section and stress due to torsion in the middle of one of the sides (Timoshenko & Goodier, 1934).

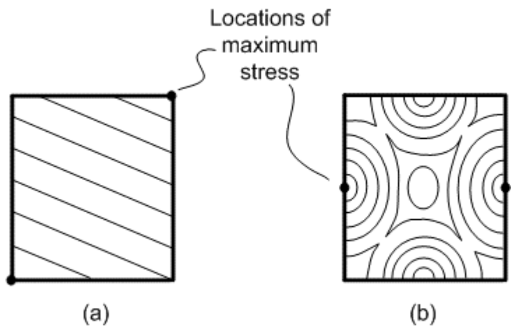

Figure 23 Stress contours for rectangular cross sections due to bending (a) and torsion (b)

Two unity checks are made to ensure sufficient capacity to resist double bending:

$$k_m \frac{\sigma_{m,y,d}}{f_{m,y,d}} + \frac{\sigma_{m,z,d}}{f_{m,z,d}} \leq 1$$

$$\frac{\sigma_{m,y,d}}{f_{m,y,d}} + k_m \frac{\sigma_{m,z,d}}{f_{m,z,d}} \leq 1$$

Where:

$$k_m = 0.7$$

If one of these checks is violated at a certain grid point action is taken to alter the position of this grid point such that stresses decrease as described in chapter 2. If in the final equilibrium position the stresses at the grid point do still not satisfy the two checks, an entry in the report will be written by the design tool.

If torsion, shear and axial forces are considered as well, a different criterion is needed, for instance (Toussaint, 2007):

$$\left(\frac{\sigma_{m,d}}{f_{m,d}}\right)^2 + \left(\frac{\tau_{v,d}}{f_{v,d}}\right)^2 + \left(\frac{\sigma_{c/t,0,d}}{f_{c/t,0,d}}\right)^2 \leq 1$$

Where:

$$\sigma_{m,d} = \sigma_{m,y,d} + \sigma_{m,z,d}$$

$$\tau_{v,d} = \tau_{xy,d} + \tau_{tor,d}$$

Stress due to actions other than bending is not taken into account by the developed design tool, because bending is considered to have the most important effect. However, in theory it is very well possible to implement all other effects with a similar approach as used for bending.

3.4.3. Mannheim grid shell

To test if the developed design tool works properly, it is applied to a test case based on the Mannheim grid shell. From the documentation of the Institut für leichte Flächen-tragwerke (Burkhardt et al, 1976) the following information can be obtained on the Mannheim grid shell:

Timber properties:

Wood species: Western Hemlock

Mean bending strength: 83.0 N/mm^2

Standard deviation of bending strength: 20.6 N/mm^2

Mean modulus of elasticity: 10400 N/mm^2

From this for the characteristic bending strength can be found as:

$$83.0 - 1.65 \times 20.6 = 49.0 \ \frac{N}{mm^2}$$

To take into account any imperfections that may exist in the timber a value of 40.0 N/mm^2 will be used.

Use was made of a double layered grid built-up of two sets of 50x50mm laths:

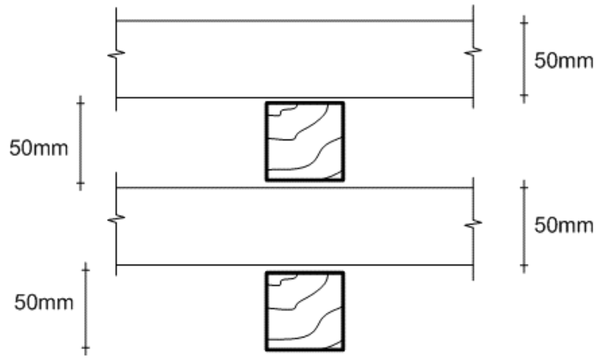

Figure 24 *Grid point connection Mannheim*

The two sets of laths were free to move relative to each other during erection. Since the laths were not connected the occurring stresses corresponded to that of a single 50x50mm lath being bent into shape.

The four required variables for the stress check can therefore be specified as:

$E_{0,mean}$ = 10.4 kN/mm^2

$f_{m,k}$ = 40.0 N/mm^2

b = 50.0 mm

h = 50.0 mm

```
22                (-)     Number of gridpoints direction i
20                (-)     Number of gridpoints direction j
1.2               (m)     Distance between gridpoints

0.90              (s)     Timestep for numerical integration
1.0               (kg)    Virtual mass of particles
100000000.        (N/m)   Spring stiffness axial springs stage 1
10000000.         (N/m)   Spring stiffness axial springs stage 2
8000000.          (N/m)   Spring stiffness shape springs
0.000000001500    (kg/s)  Damping constant stage 1
0.000000016000    (kg/s)  Damping constant stage 2
0.9              (-)     Reduction factor shape springs
1.0               (N)     Maximum mean of force resultants on grid points stage 1
1000.0               (N)     Maximum resultant of forces on any one grid point stage 2

400.0             (kg/m3)  Density of timber
10.4              (kN/mm2) Elastic modulus (E_0,mean)
50.0              (mm)     Width of cross section
50.0              (mm)     height of cross section
40.0              (N/mm2)  Characteristic bending strength (f_m,k)
0.5               (-)      Relaxation factor

1   Three dimensional view   (Set desired view to '1' and other two to '0')
0   Top view
0   Front view
```

Figure 25 Input values of variables

The span/height ratio of the Mannheim grid shell ranges between 3.2 and 3.8 for the different parts of the grid shell. Based on this information a simple test case is made of a ellipsoid with a span/height ratio of 2.5 approximately. To obtain this shape the laths would have to be bent more than they do in the Mannheim grid shell. It can be expected that the shape that will be found by the design tool will have a span/height ratio in between that of the test target shape and of the actual grid shell in Mannheim.

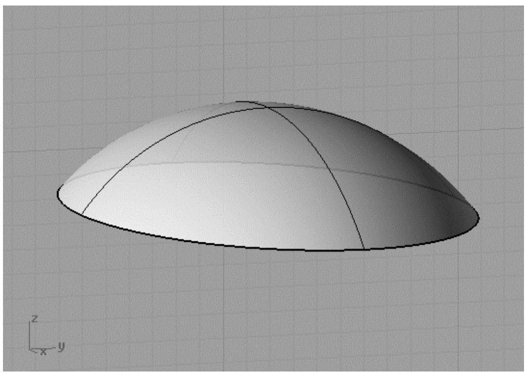

Figure 26 Target shape test case Mannheim grid shell

The span/height ratio should be smaller than or equal to that of the Mannheim grid shell, because we know that the rotations corresponding to that ratio are possible in reality.

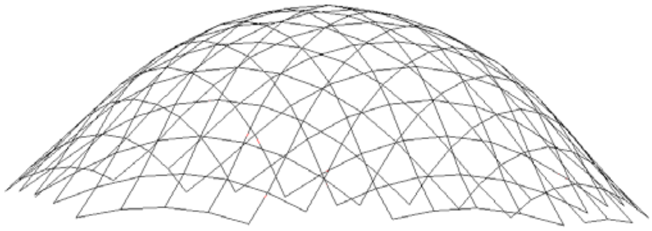

Figure 27 *Output shape design tool*

It turned out that a shell with span/height ratio of about 3.0 is found. This is what was expected to find, because it means that the rotations in the members are a bit larger than they are in the Mannheim grid shell. According to the design tool the maximum rotations that are possible are a bit bigger than those in the Mannheim grid shell. From the report written by the design tool it follows that the maximum stress is exceeded only at one grid point and only by a very small margin (most critical unity check equal to 1.003).

3.4.4. Post-construction stage

After construction has been completed other loads have to be considered and checked according to the standards. Examples are loads from wind, snow and weight from cladding material. The bending moments that resulted from the erection of the grid shell also remain present and cause additional stresses in the timber. Since they are calculated for every grid point by the design tool, it is known how large the remaining bending moments are directly after construction has been completed. However, due to relaxation the bending moments will decrease until approximately 50% remains. These remaining bending moments are given in a table in the report written by the design tool after it has finished calculations so they can be applied as an additional load case in any further checks.

3.5. Limitations

The design of timber grid shells is a very complex process, therefore in the development of the design tool certain aspects had to be simplified. The applicability of the design tool is thus bound to some limitations and constraints.

- Only one orientation of the grid is checked
- Torsion and shear are not taken into account
- Only rectangular cross sections of laths are possible
- Only equidistant grids can be considered
- No differentiation in timber properties possible through the grid

4 Evaluation

The results produced by the design tool have to be checked in order to know if they are accurate. The geometrical data of the grid points, produced by the design tool for a certain test case, are therefore compared with results that were found using the concept of minimum potential energy and with results obtained with an established software package called *Oasys GSA*. Furthermore, the results from the shape approximation procedure are checked for a given example.

4.1. Equilibrium in two dimensions

The process of finding a shape for which the internal axial- and bending forces are in equilibrium with its support reactions is fundamental for the design tool. Therefore the results of this process are checked for the basic two-dimensional case of a single beam. This single two-dimensional beam can be seen as a building block that the overall model of the timber grid shell is built up of. If it is ensured that this is modelled correctly this makes it likely that the results for more complex case will also be correct.

4.1.1. Test case

In order to set up the test case, first the design tool is used to model a beam with arbitrarily chosen properties. The beam is deformed as it would be for an arbitrary target shape and subsequently the equilibrium shape is found by the design tool with no external loading applied. From the output of the design tool the horizontal support reactions (vertical support reactions are virtually zero) at the two endpoints follow, together with the grid point coordinates.

The design tool is set to model the lath by creating grid points at a distance of 0.2m apart and to stop iterating once the force resultant is less than 0.05N for every grid point. In this way the following set of values is obtained for the test case:

- Length of beam 7.6 m
- Flexural rigidity (EI) 95000 Nm^2
- Horizontal support reactions 18093 N

These same values will be used in the analytical model and in *Oasys GSA* to see how the shape of the beam compares under similar loading conditions and beam properties.

4.1.2. Minimum potential energy

To gain understanding in the bending behaviour of the laths in the timber grid shell the deformation of a single lath is examined analytically. An appropriate way to find the shape a beam will take on under a certain load is to use the concept of minimum potential energy. This method is therefore applied to the test case derived from results found with the design tool.

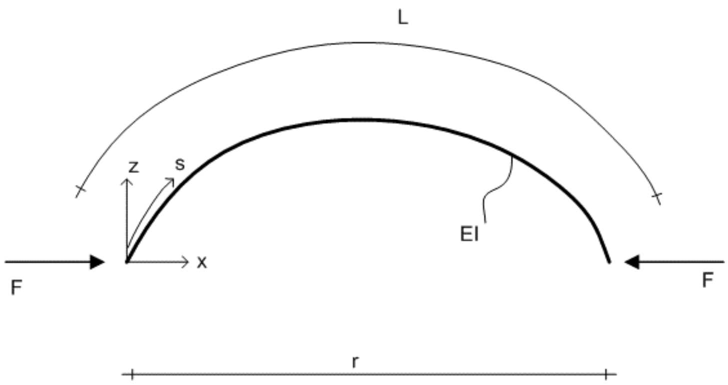

Figure 28 Beam deformed by horizontal loads

It is assumed that the deflection of the beam as a function of *s* (which is a parameter that runs along the developed length of the lath) can be described as the sum of goniometric terms. A suitable example of such a function is:

$$w(s) = a \times \sin\left(\frac{s\pi}{L}\right) + b \times \sin\left(\frac{3s\pi}{L}\right)$$

In Figure 29 the two terms of this function are depicted separately (with a = b = 1).

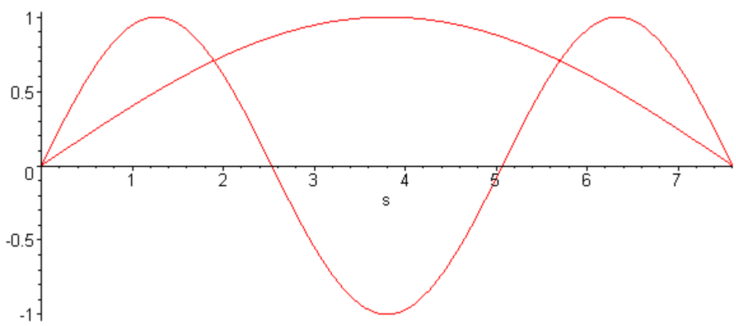

Figure 29 Two terms of the assumed function describing the shape of the lath

The values of *a* and *b* need to be found for which the system has a minimum in its potential energy. This corresponds to the equilibrium situation for the given beam properties and loading conditions. It should be noted that the correctness of the solution depends on how well the initially assumed function was chosen.

The potential energy of the system is given by:

$$E_{pot} = \frac{EI}{2} \times \int_0^L \kappa^2 \, ds - F(L-r)$$

Where

$$\kappa = \frac{\frac{d^2w}{ds^2}}{\sqrt{1-\left(\frac{dw}{ds}\right)^2}}$$

These functions can be evaluated (by computer) for different values of *a* and *b* to find for which combination of the two the potential energy is at a minimum. It turned out that this is the case for:

- *a* = 2.01
- *b* = -0.0280

(See appendix for the *Maple* sheet used for the calculations)

All parameters in the assumed function are now defined and the function can be evaluated at all the values of *s* that correspond to the grid points used in the design tool.

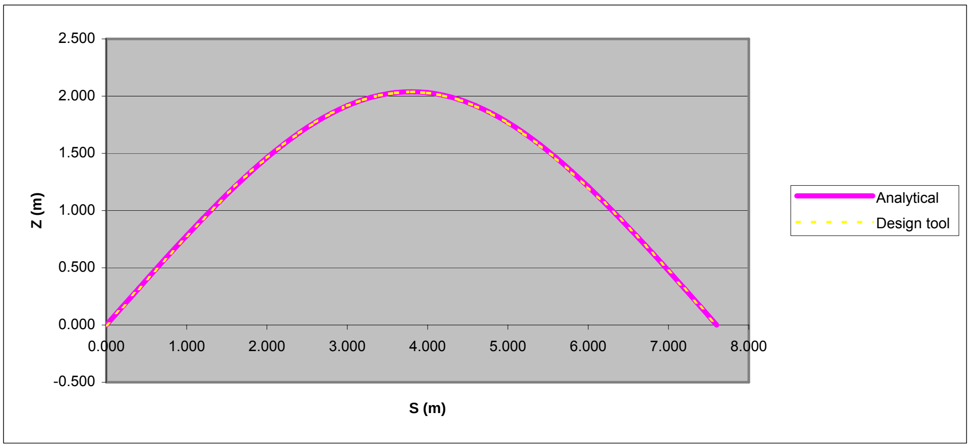

Figure 30 Deflections analytical approach and design tool

From Figure 30 it is clear that the overall shape compares very well with the shape found by the design tool.

4.1.3. Oasys GSA

Another way of finding the equilibrium shape of a deformed beam is by using available software that is used in practice. One such programme is *Oasys GSA* which uses dynamic relaxation to solve non linear systems. *Oasys GSA* is used to model the lath of the test case again. The beam is divided into sections that correspond to the distance between the grid points used in the design tool (0.2m). The lath is given a small initial deformation to make sure the programme will look for equilibrium of a deformed shape. The iteration process is set to stop the sum of all force resultants on the grid points (called the residue of forces) is less than 0.001% of the total applied load.

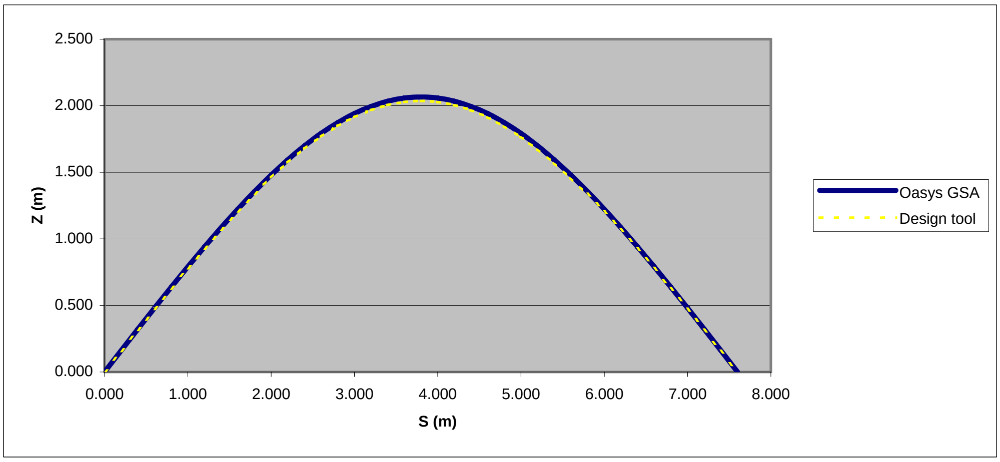

Figure 31 Deflections design tool and Oasys GSA

Again the positions of the grid points seem to correspond well with the positions of the grid points found by the design tool.

4.1.4. Comparison of deflections

In Figure 32 the difference between the deflections found by the design tool and the other two methods is shown.

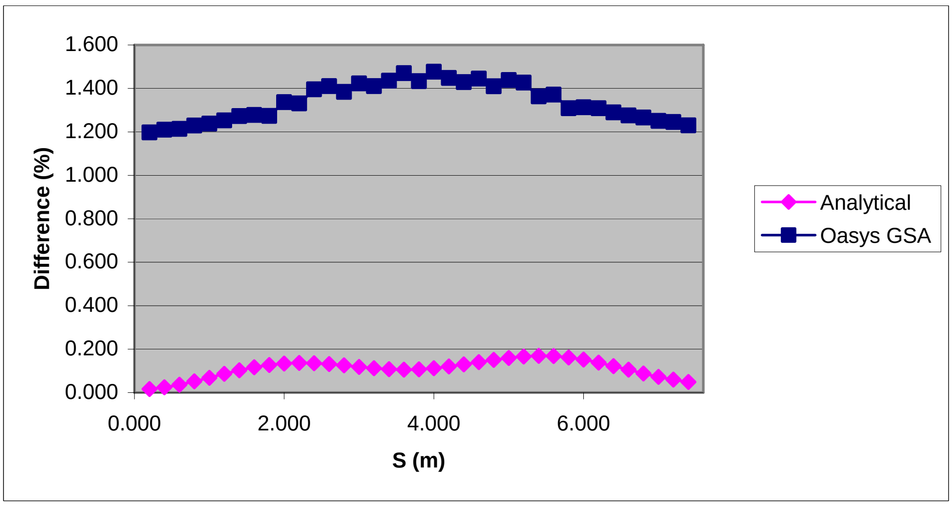

Figure 32 Comparison of results

It can be seen that the deflections are bigger in the other two methods, although the differences are minimal. An explanation for the less stiff behaviour is that the design tool considers the distance between grid points as straight lines, whereas the other two methods take into account the actual shape of the lath in between the grid points. This leads to an underestimate for the rotational spring stiffness at the grid points since this is calculated by lumping together the flexural rigidity of the lath material in between grid points.

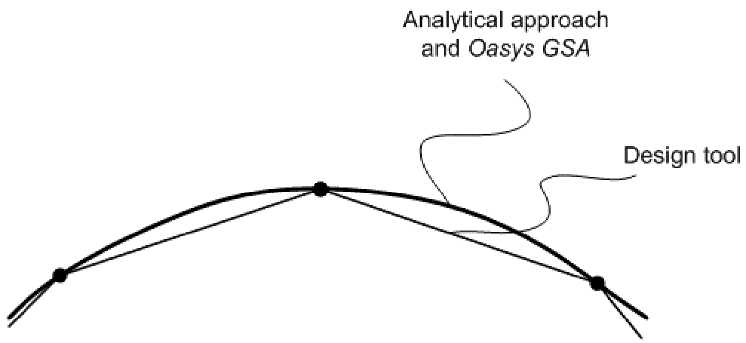

Figure 33 Lath in between the grid points

Since differences between the deflections found by the design tool and the other two methods are very small it can be assumed that the formulas used to model the bending and extension/compression behaviour in the design tool are correct and correctly implemented.

4.2. Equilibrium in three dimensions

In three-dimensional grids additional effects play a role. Since the laths in perpendicular directions will interact it has to be checked if the results in three dimensions are still reliable. The design tool does not have torsion behaviour implemented, so the effects of this have to be investigated as well.
Finding an analytical solution for even a simple three-dimensional grid is very difficult, so the results are only compared with results obtained from *Oasys GSA* for the same geometry and loading conditions.

4.2.1. Test case

A simple test case is set up of a square grid with 169 nodes. At the node at the centre a point load is applied. This node is constrained in the x- and y-directions. The nodes at the perimeter are constrained in the z-direction. All other nodes are unconstrained.
Input values:

- Elastic modulus ($E_{0;mean}$): 10.4 kN/mm^2
- Width of cross section: 50 mm
- Height of cross section: 50 mm
- Point load: 50 kN
- Grid point distance: 0,5 m

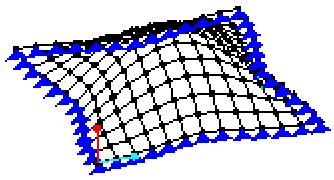

Figure 34 Test case in the design tool

The design tool is modified such that the shape approximation is omitted. The design tool is set to run until finding equilibrium.

4.2.2. Oasys GSA

In Oasys GSA the grid is again set up with equal properties as before and with equal loading and support conditions.

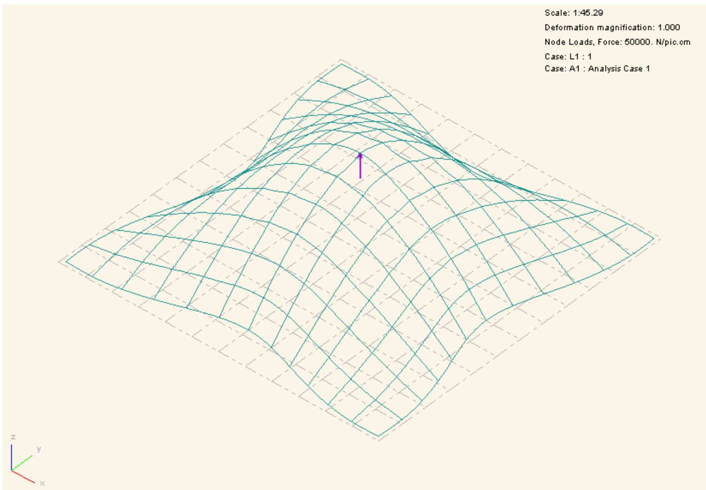

Figure 35 Test case in Oasys GSA

It appears that both applications come up with a shape that is very similar. The maximum displacement of the grid point at the centre is about 1.7 metre upward, and the grid points at the middle of the edges will displace about 0.7 metre inwards. This is true for both the results found by the design tool and the result found by *Oasys GSA*.

In order to compare the results more specifically, the results are investigated further. Both the design tool and *Oasys GSA* find a certain shape of the surface defined by the geometry of the nodes. The positions of these nodes are defined by their x-, y- and z-coordinates. By taking the total distance in space between every grid point position found by the design tool and its counterpart found by *Oasys GSA* a surface can be created that depicts the difference between the two solutions.

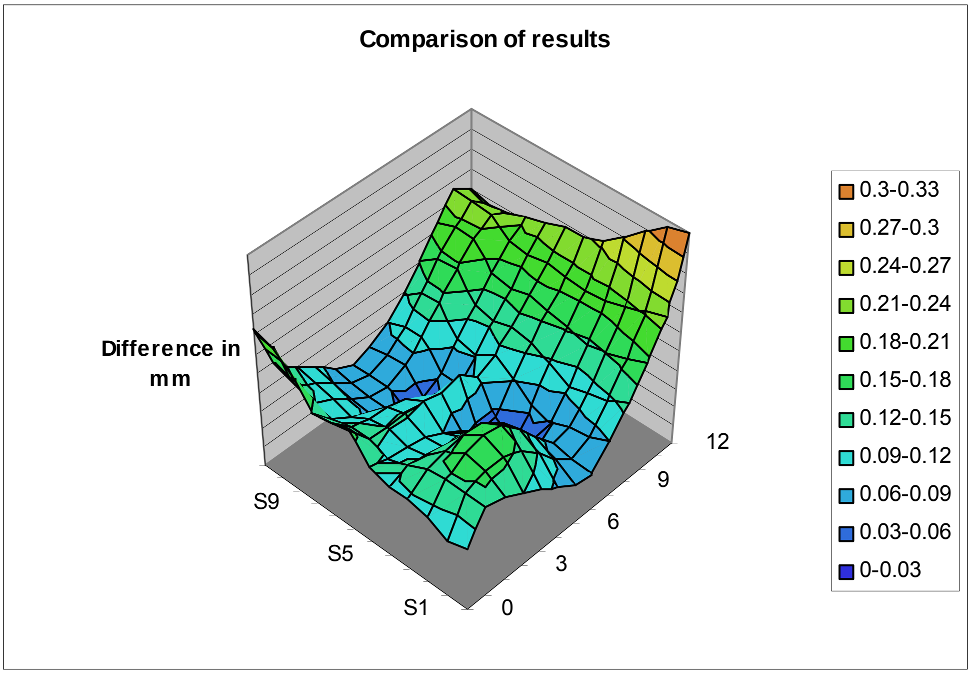

Figure 36 *Difference between the surfaces found by of the design tool and Oasys GSA*

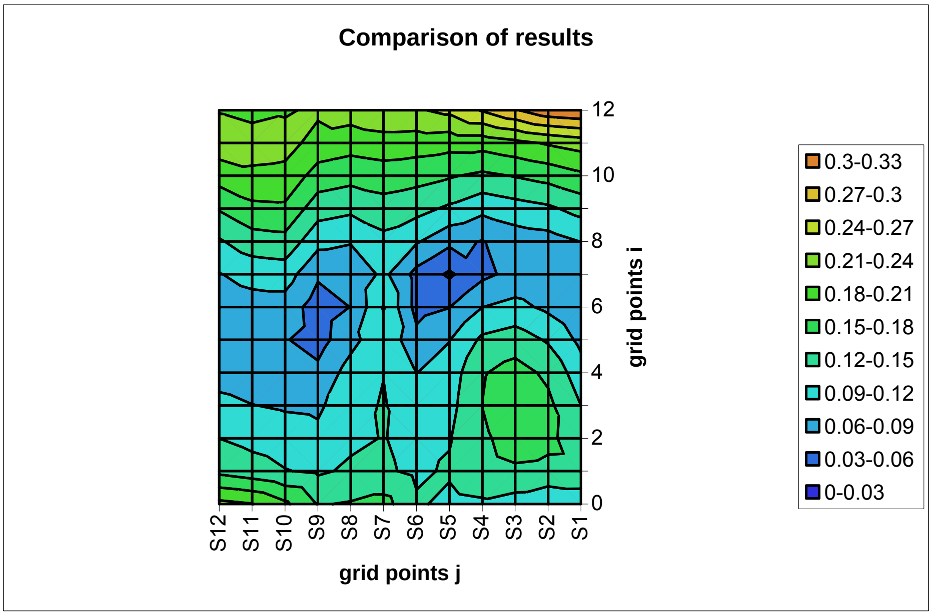

Figure 37 *Projected view of the differences*

It turns out that the results compare quite well. The maximum difference between a grid point in the result found by the design tool and its counterpart as found by *Oasys GSA* is 328 mm. The differences are largest at the edges and decreasing towards the centre, this can be the result of a difference in rotation of the grid as a whole around the grid point in the centre.

If only the z-components of the positions of the grid points are compared the following figure can be obtained.

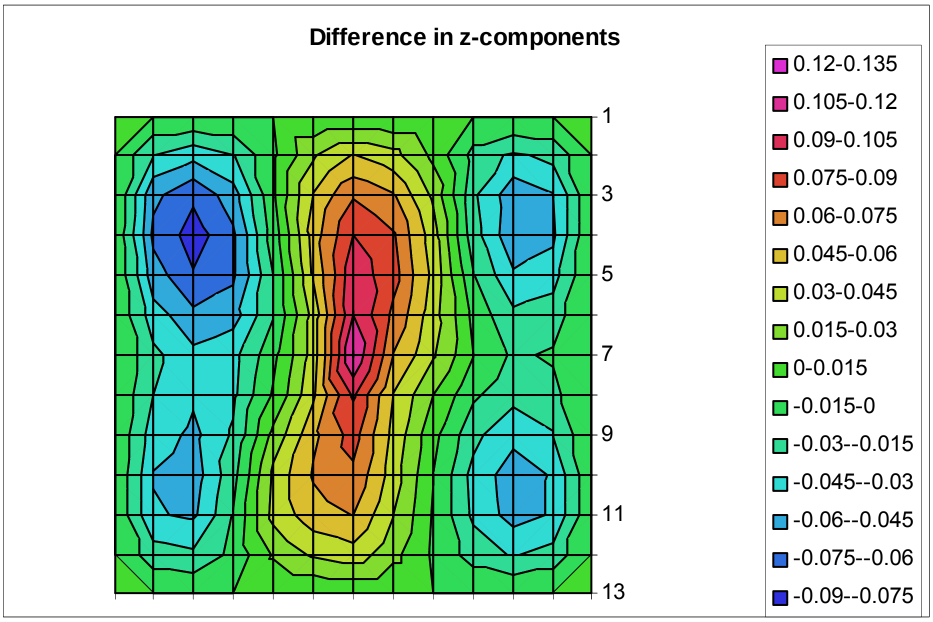

Figure 38 *Comparison of z-components of results*

Now the maximum difference is 122 mm at the grid point at the centre, which is about 7% of the total deformation at this point.

The solution procedure in *Oasys* is very similar to the procedure used in the design tool, but *Oasys* can be expected to be more accurate, because it takes more aspects into account, including torsion behaviour. This can be the explanation for the difference in results. Overall the deflection found is very similar, so it can be concluded that the design tool gives good results, but that an error of about 10% can be present in the results.

4.3. Shape approximation

The general goal of the shape approximation process is to find a shape that is as close to the target shape as possible without exceeding the limitations on stresses in the timber. If this stress is too large the shape of the grid shell has to be altered such that the stress at that location is reduced.

In the developed design tool only stresses due to bending are checked. The output shape is altered if the stresses do not satisfy the limits required by NEN-EN1995-1-1. In this case the vertical force used to deform the laths conform the target shape is reduced, which generally leads to a reduction in the bending moments.

When looking at two-dimensional shapes, this procedure can be considered to work correctly when grid points that are not on the target shape have a certain maximum curvature that corresponds to a stress state that is just within limits.

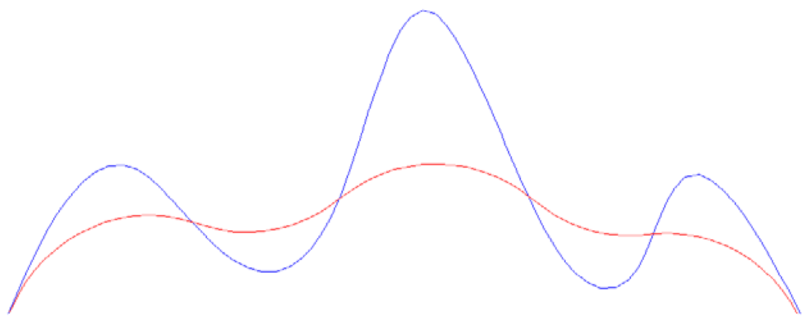

Figure 39 Target shape and output shape after shape approximation

For example with the target shape as depicted in Figure 39 (in blue) this implicates that the curvature in the output shape (in red) should almost everywhere be equal to this maximum curvature because the output shape is not on the target shape anywhere apart from at the points of inflection. This appeared to be true for the depicted target shape and several others. It can therefore be concluded for the two-dimensional case that the shape found during the shape approximation process satisfies all the requirements.

In three dimensions the procedure works less well. It turns out that the average of the most critical unity check for all the grid points that have not moved away from the target shape is about 0.86 for a certain test case. The average unity check of the grid points that have not moved away from the target shape is 0.8. The stresses in the grid points that have moved away from the target shape are indeed more critical, which justifies why those grid points moved away from the target shape. However, ideally the design tool would come up with a geometry where unity checks for the grid points are just under 1.0, so 0.99 instead of 0.86. This difference results from the fact that when out-of-plane bending is too large, the stresses resulting from this do not decrease when the vertical shaping force is reduced. The shape approximation of the developed design tool is not fully accurate, but it can be concluded that the approach used can lead to good results if the method described in the previous chapter is worked out further into the design tool.

5 Case study

In this chapter the general procedure is described for a given example of how the developed design tool can be used within the overall design process of a timber grid shell.

The first step is to come up with a suitable shape of a shell like structure. Although the design tool will always find a shape for the timber grid shell, whatever the input shape you first specify, the better this initial shape resembles a structural shell, the better the final result will look like the original. The initial design can still consist simply of a collection of basic shapes that conform to the basic interior space requirements of the envisioned shell structure since the design tool will drape a continuous grid over it.

One of the available software packages that is commonly used in practice is *Rhinoceros*. For this case study this is used to draw a possible shell that consists of three ellipsoids merged together to form a hall of about 30 metre length, 20 metre width and 5 metres high.

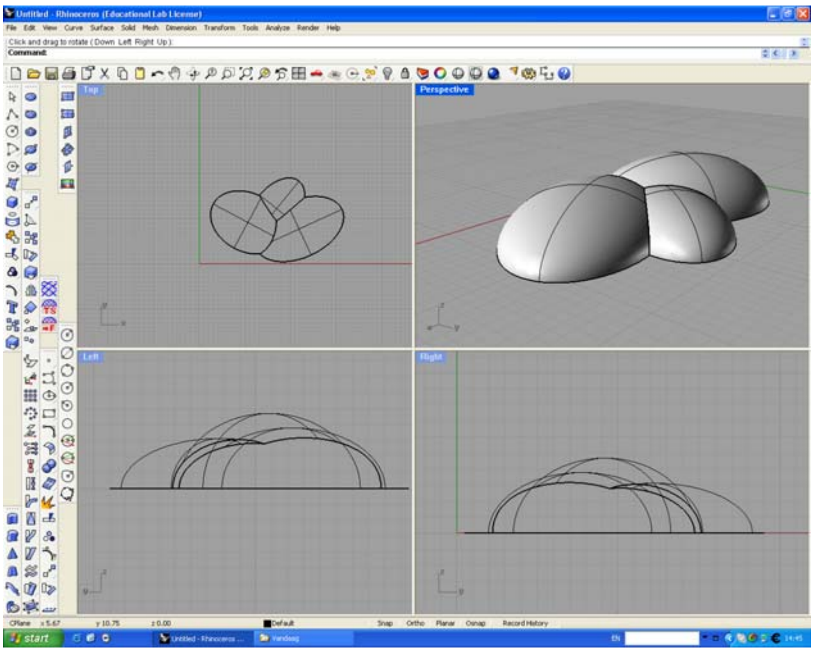

Figure 40 Drawing of initial shape in Rhinoceros

In order for the developed design tool to be able to work with the specified shape, it needs to be discretisised to points. In *Rhinoceros* there is a function for this called *DrapePt*, which will draw points onto the surface. There has to be a sufficient umber of points drawn to define the shape properly.

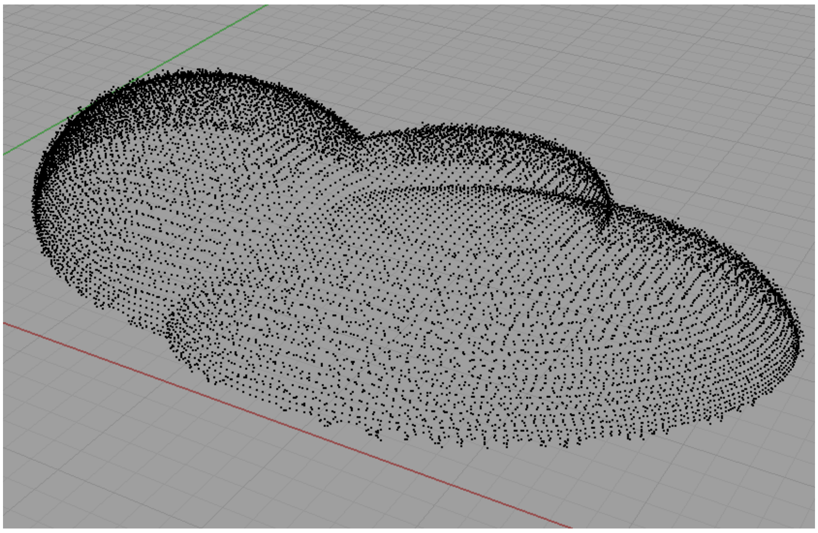

Figure 41 *Shape defined by points in Rhinoceros*

By saving the coordinates of these points to a text file with the name 3Dgeometry.txt the input shape is ready to be used in the design tool. Every point of the shape needs to be specified on its own line and the x- , y- and z-coordinates have to be separated by spaces. Rhinoceros can do all this automatically, when the points file export options are specified as shown in Figure 42.

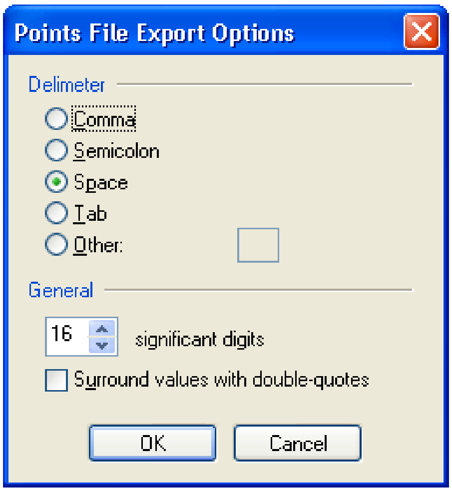

Figure 42 *Points file export in Rhinoceros*

An example of the resulting text file can be seen in Figure 43. The file can contain up to a million points.

3Dgeometry.txt - Notepad

```
16.48723774404101 15.52758523389941 2.707641542487858
16.72523814877399 15.68373828760225 2.707641542487858
16.96323855350697 15.71126539262777 2.707641542487858
17.20123895823994 15.99604128986356 2.707641542487858
17.43923936297292 15.99604128986356 2.707641542487858
17.6772397677059 15.8398897887329 2.707641542487858
17.91524017243888 16.00509278576309 2.707641542487858
18.15324057717186 16.00509278576309 2.707641542487858
18.39124098190483 16.30834584469705 2.707641542487858
18.62924138663781 16.30834584469705 2.707641542487858
18.86724179137079 16.00509278576309 2.707641542487858
19.10524219610377 16.00509278576309 2.707641542487858
19.34324260083675 16.07663686510211 2.707641542487858
19.58124300556973 15.71126539262777 2.707641542487858
19.8192434103027 15.71126539262777 2.707641542487858
20.05724381503568 15.76433231026862 2.707641542487858
20.29524421976866 15.45202775543512 2.707641542487858
20.53324462450163 14.20281264124553 2.707641542487858
20.77124502923461 12.18533356985955 2.707641542487858
21.00924543396759 12.18533356985955 2.707641542487858
21.24724583870057 12.18533356985955 2.707641542487858
21.48524624343355 12.47916096299487 2.707641542487858
21.72324664816653 12.47916096299487 2.707641542487858
21.9612470528995 12.47916096299487 2.707641542487858
22.19924745763248 12.47916096299487 2.707641542487858
22.43724786236546 12.47916096299487 2.707641542487858
22.67524826709844 12.77298913241629 2.707641542487858
22.91324867183142 12.77298913241629 2.707641542487858
23.15124907656439 12.77298913241629 2.707641542487858
23.38924948129737 12.77298913241629 2.707641542487858
23.62724988603035 12.77298913241629 2.707641542487858
23.86525029076333 12.77298913241629 2.707641542487858
24.10325069549631 12.77298913241629 2.707641542487858
24.34125110022928 12.77298913241629 2.707641542487858
24.57925150496226 12.77298913241629 2.707641542487858
24.81725190969524 12.77298913241629 2.707641542487858
25.05525231442822 13.10974747561439 2.707641542487858
25.2932527191612 12.77298913241629 2.707641542487858
25.53125312389417 12.77298913241629 2.707641542487858
25.76925352862715 12.77298913241629 2.707641542487858
26.00725393336013 12.77298913241629 2.707641542487858
26.24525433809311 12.77298913241629 2.707641542487858
26.48325474282608 12.79744369706699 2.707641542487858
26.72125514755906 12.47916096299487 2.707641542487858
26.95925555229204 12.47916096299487 2.707641542487858
27.19725595702502 12.4851391422335 2.707641542487858
27.435256361758 12.4851391422335 2.707641542487858
27.67325676649097 12.18533356985955 2.707641542487858
```

Figure 43 Coordinates of points on input shape

The next step is to specify the input variables in another text file called Input.txt. This input file needs to be in the same format as depicted below. Apart from the values of the numbers nothing should be changed in this file, otherwise the design tool is no longer capable of reading its contents.

Input.txt - Notepad

```
50                  (-)        Number of gridpoints direction i
50                  (-)        Number of gridpoints direction j
1.0                 (m)        Distance between gridpoints


0.90                (s)        Timestep for numerical integration
1.0                 (kg)       Virtual mass of particles
100000000.          (N/m)      Spring stiffness axial springs stage 1
10000000.           (N/m)      Spring stiffness axial springs stage 2
8000000.            (N/m)      Spring stiffness shape springs
0.000000001500      (kg/s)     Damping constant stage 1
0.000000016000      (kg/s)     Damping constant stage 2
0.95                (-)        Reduction factor shape springs
1.0                 (N)        Maximum mean of force resultants on grid points stage 1
0.01                (N)        Maximum resultant of forces on any one grid point stage 2


400.0               (kg/m3)    Density of timber
10.4                (kN/mm2)   Elastic modulus (E_0,mean)
50.0                (mm)       Width of cross section
50.0                (mm)       Height of cross section
41.8                (N/mm2)    Characteristic bending strength (f_m,k)
0.5                 (-)        Relaxation factor


1    Three dimensional view   (Set desired view to '1' and other two to '0')
0    Top view
0    Front view
```

Figure 44 Input variables

It is important that the initial grid is large enough to completely drape around the input shape. Therefore the numbers of grid points should not be taken too small. However by taking it too large the design tool will become unnecessarily slow.
The input variables are divided into four groups. The first three variables determine the initial shape of the grid, the next ten variables can be adjusted to influence the calculation procedure. After that follow six variables that specify the timber behaviour, and the last three variables specify how the process has to be visualised.
The variables that specify the calculation process generally don't have to be altered. However if for some reason someone would like to see what happens if the spring stiffness of the axial springs is given a different value, the damping constant needs to be adjusted as well in order to prevent the calculation from becoming unstable.
Once all the values in the input file are given the desired value and the 3Dgeometry.txt and Input.txt files are placed into the same folder as the timber grid shell design tool application everything is ready to start the calculation by clicking the design tool icon.

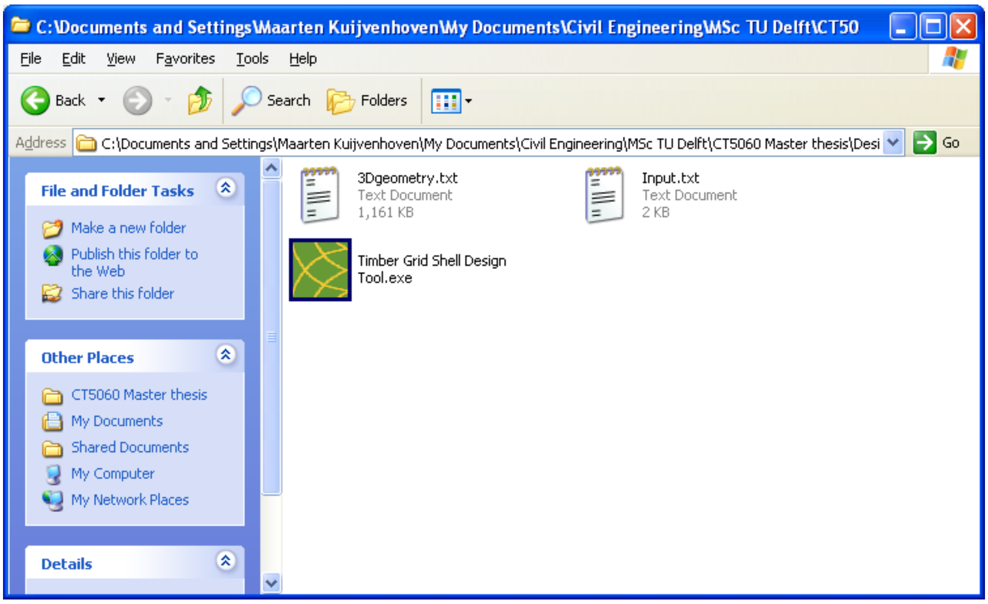

Figure 45 Folder with the design tool application and the two required input files

The design tool will now start iterating and its progress can be observed. After some time the design tool will have found equilibrium and stops iterating. It will then write a report and save the coordinates of the grid points to a file with the dxf format.

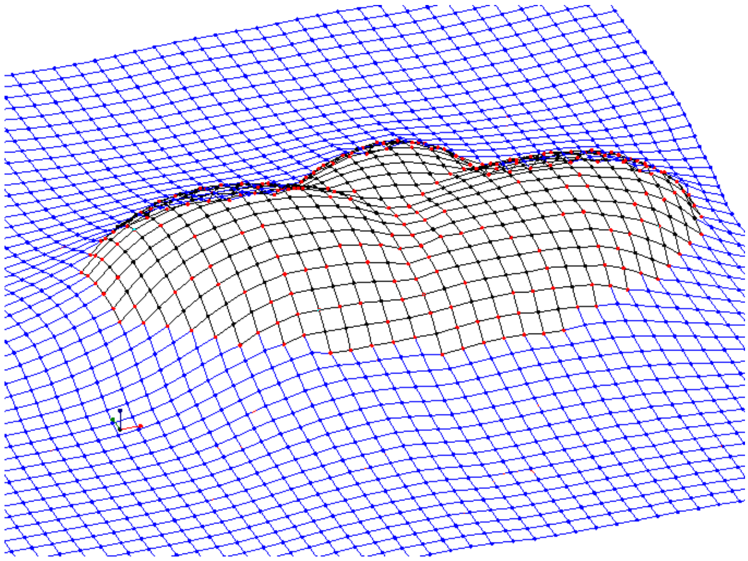

Figure 46 *The design tool during calculation*

An example of a report can be found in Appendix C: Report example. The dxf file can be used for further analysis with other software.

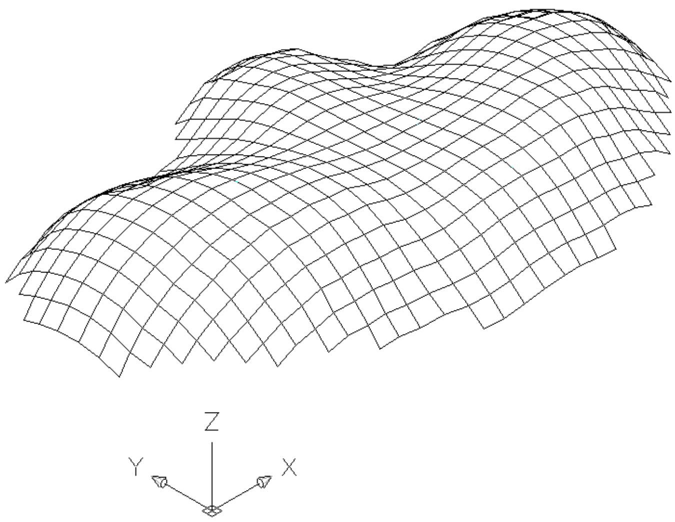

Figure 47 *The geometry of the timber grid shell as found by the design tool*

The geometry of the grid shell as it is specified should be further analysed and adjusted before it can actually be build. Most engineering software can work with the dxf format, including the *Oasys GSA* package.

Bending moments will remain in the timber after construction, an indication of these are given in the report as a table with the expected remaining bending moments for every grid point. These should be applied as an additional load case to the structure.

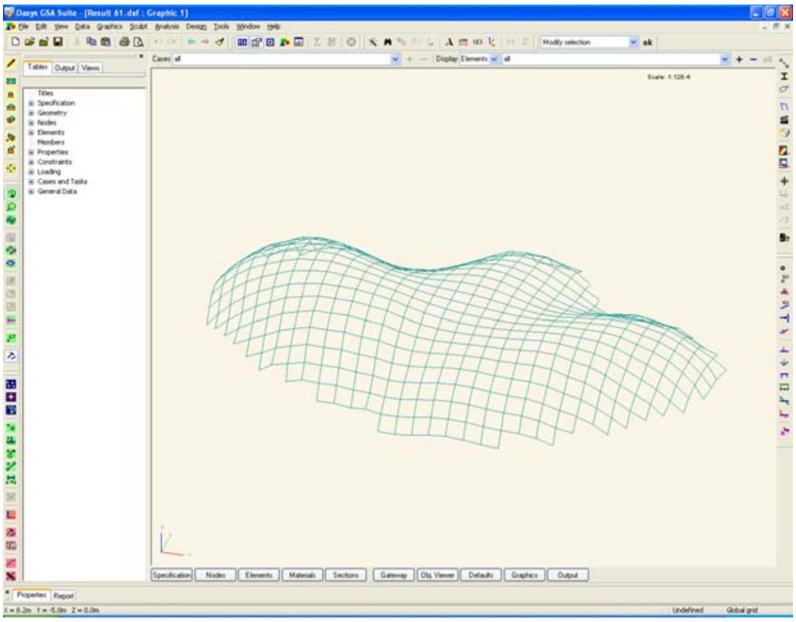

Figure 48 *Further analysed in Oasys GSA*

6 Conclusions and recommendations

Conclusions:

- The behaviour of a timber grid shell during construction can be simulated by a discrete model consisting of particles and springs.
- The development of design tools for timber grid shells has large potential, because it can make use of computational power to help determine the equilibrium shape.
- Despite its elementary approach, the developed design tool is demonstrated to give generally satisfactory results.
- It is difficult to build a design tool that can find the best possible shape that conforms to all demands due to the separate form finding stage and stress checking stage.
- With the developed design tool it is not necessary to define the initial shape very accurately, instead it can be build up of basic components like ellipsoids, cylinders etc. The tool will drape a grid around it to find a continuous shell structure.

Recommendations on further work on the developed design tool:

- The rotation of the laths along their length should be implemented by considering a local reference system.
- Torsion and shear stresses should be modelled and checked by implementing corresponding spring systems.
- Material behaviour in between grid points can be modelled more realistically.
- More attention should be paid to how the supports are created.
- To improve the speed and numerical stability dynamic relaxation with kinematic damping should be implemented.
- The design tool can only find a shape for a given orientation of the grid. It would be beneficial if the tool was capable to investigate several orientatios.
- The application of safety factors in the design have to be considered which also take into account the limitations that result from the set-up of the design tool.
- Other materials then timber, such as glass fibre composites or even cardboard (Douthe, 2006), may be even more applicable for the construction of grid shells.

Appendix A: Maple sheet used for validation

```
> restart;
> with(plots):
> w:=a*sin(s*Pi/L)+b*sin(s*3.*Pi/L);
```

$$w := a\sin\left(\frac{s\,\pi}{L}\right) + b\sin\left(\frac{3.\,s\,\pi}{L}\right)$$

```
>
> kappa:=diff(w,s,s)/sqrt(1.-diff(w,s)^2);
```

$$\kappa := \frac{-\dfrac{a\sin\left(\frac{s\,\pi}{L}\right)\pi^2}{L^2} - \dfrac{9.\,b\sin\left(\frac{3.\,s\,\pi}{L}\right)\pi^2}{L^2}}{\sqrt{1. - \left(\dfrac{a\cos\left(\frac{s\,\pi}{L}\right)\pi}{L} + \dfrac{3.\,b\cos\left(\frac{3.\,s\,\pi}{L}\right)\pi}{L}\right)^2}}$$

```
> F:=18093.;          # zoals gevonden met design tool
```

$$F := 18093.$$

```
> L:=7.6;
```

$$L := 7.6$$

```
> EI:=95000.0;
```

$$EI := 95000.0$$

```
> display({plot(sin(s*Pi/L),s=0..L),plot(sin(s*3.*Pi/L),s=0..L)});
```

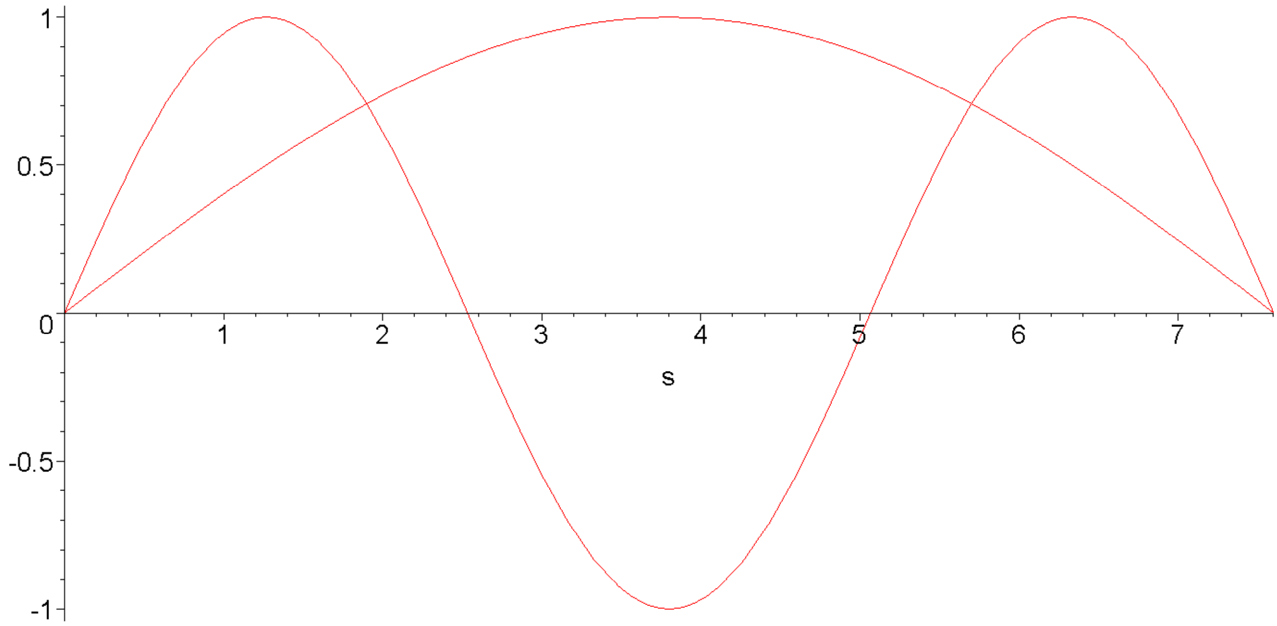


```
> w:=eval(w);
```

$$w := a\sin(0.1315789474\,s\,\pi) + b\sin(0.3947368422\,s\,\pi)$$

```
> kappa:=eval(kappa);
```

$\kappa := ($

$-0.01731301939\,a\sin(0.1315789474\,s\,\pi)\,\pi^2 - 0.1558171745\,b\sin(0.3947368422\,s\,\pi)\,\pi^2)$

$/ \,($

$$1. - (0.1315789474\, a \cos(0.1315789474\, s\, \pi)\, \pi + 0.3947368422\, b \cos(0.3947368422\, s\, \pi)\, \pi)^2)^{(1/2)}$$

```
> r:=evalf(eval(Int(sqrt(1.-diff(w,s)^2),s=0..L)));
```

$$r := \int_{0.}^{7.6} \sqrt{1. - 1.\, (0.4133674546\, a \cos(0.4133674546\, s) + 1.240102364\, b \cos(1.240102364\, s))^2}\, ds$$

```
> Epot:=evalf(eval(EI/2.*Int(kappa^2,s=0..L)))-F*(L-r);
```

$$Epot := 47500.00000 \int_{0.}^{7.6} \frac{(-0.1708726524\, a \sin(0.4133674546\, s) - 1.537853872\, b \sin(1.240102364\, s))^2}{1. - 1.\, (0.4133674546\, a \cos(0.4133674546\, s) + 1.240102364\, b \cos(1.240102364\, s))^2}\, ds$$
$$- 137506.8 + 18093. \int_{0.}^{7.6} \sqrt{1. - 1.\, (0.4133674546\, a \cos(0.4133674546\, s) + 1.240102364\, b \cos(1.240102364\, s))^2}\, ds$$

```
> b:=-0.0280;
```

$$b := -0.0280$$

```
> plot(Epot,a=1.97..2.05,P=-1496..-1480,axes=BOXED);
```

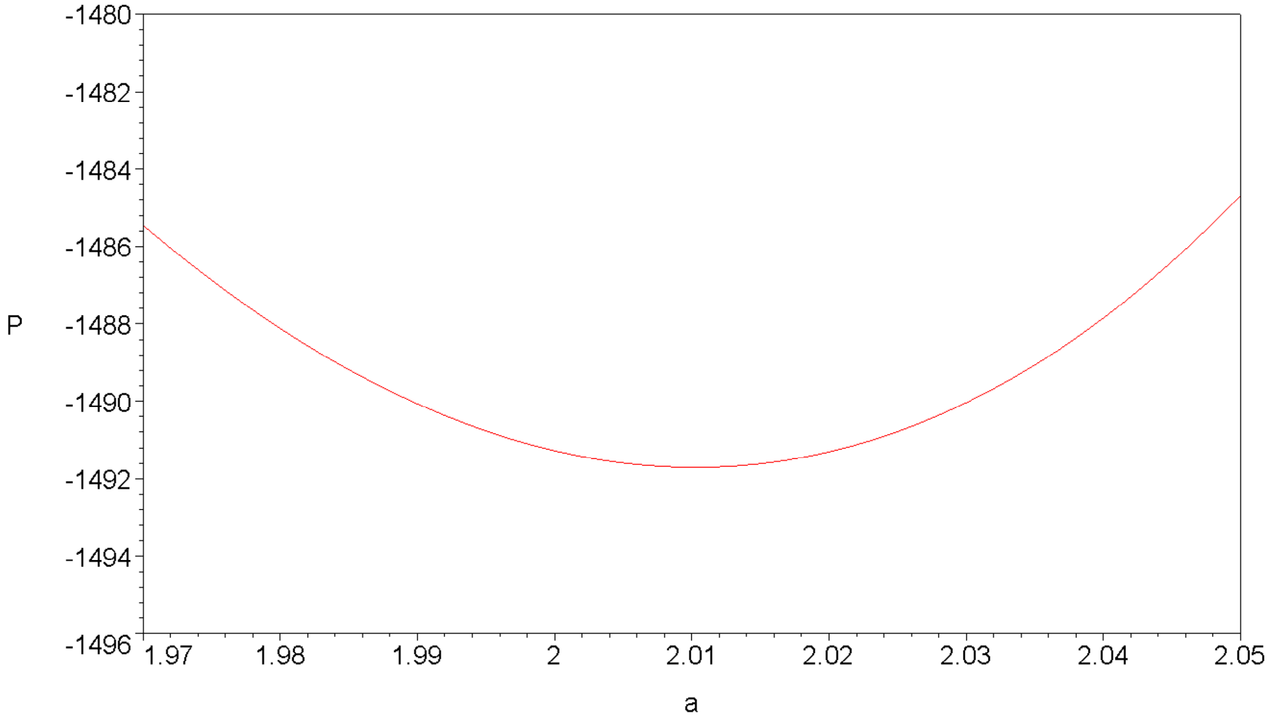


```
> assign(solve(diff(Epot,e)=0));
> a:=2.01;        # afgelezen uit bovenstaande grafiek
```

$$a := 2.01$$

```
> w:=evalf(w);
```

$$w := 2.01 \sin(0.4133674546\, s) - 0.0280 \sin(1.240102364\, s)$$

```
> plot(w,s=0..L,scaling=CONSTRAINED);
```

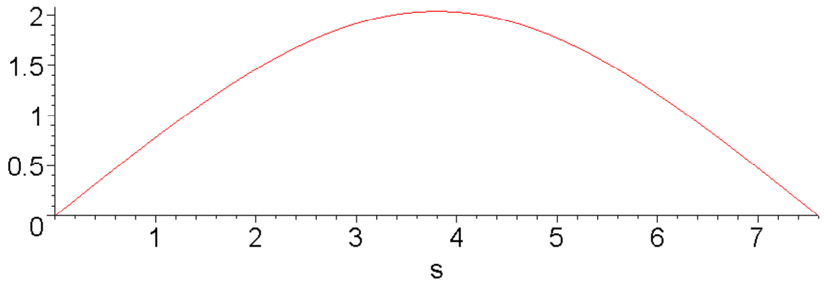


```
> r:=evalf(r);
```

$$r := 6.054510733$$

```
> gridspacing:=0.2;
```

$$gridspacing := 0.2$$

```
> for j from 0. by gridspacing to L do eval(w(s),s=j) end;
>
```

0.

0.1591108909

0.3175085995

0.4744619455

0.6292052721

0.7809249210

0.9287498945

1.071747682

1.208925900

1.339240026

1.461607105

1.574924952

1.678095974

1.770054462

1.849795972

1.916407204

1.969094805

2.007211485

2.030278038

2.0380

2.030278038

2.007211485

1.969094803

$$1.916407203$$
$$1.849795971$$
$$1.770054461$$
$$1.678095971$$
$$1.574924950$$
$$1.461607103$$
$$1.339240023$$
$$1.208925897$$
$$1.071747678$$
$$0.9287498929$$
$$0.7809249193$$
$$0.6292052700$$
$$0.4744619432$$
$$0.3175085972$$
$$0.1591108883$$
$$-0.2688058224\ 10^{-8}$$

>

Appendix B: Input variables

50	(-) Number of gridpoints direction i
50	(-) Number of gridpoints direction j
1.0	(m) Distance between gridpoints
0.90	(s) Timestep for numerical integration
1.0	(kg) Virtual mass of particles
100000000.	(N/m) Spring stiffness axial springs stage 1
10000000.	(N/m) Spring stiffness axial springs stage 2
8000000.	(N/m) Spring stiffness shape springs
0.000000001500	(kg/s) Damping constant stage 1
0.000000016000	(kg/s) Damping constant stage 2
0.95	(-) Reduction factor shape springs
1.0	(N) Maximum mean of force resultants on grid points stage 1
0.01	(N) Maximum resultant of forces on any one grid point stage 2
400.0	(kg/m3) Density of timber
10.4	(kN/mm2) Elastic modulus (E_0,mean)
50.0	(mm) Width of cross section
50.0	(mm) Height of cross section
41.8	(N/mm2) Characteristic bending strength (f_m,k)
0.5	(-) Relaxation factor

1	Three dimensional view (Set desired view to '1' and other two to '0')
0	Top view
0	Front view

Appendix C: Report example

```
*********************************************************
**                                                     **
**   Design Tool for Timber Grid Shells                **
**                                                     **
**   Maarten Kuijvenhoven                              **
**   Delft University of Technology                    **
**                                                     **
*********************************************************
```

Input parameters:

20 Number of gridpoints direction i (-)
20 Number of gridpoints direction j (-)
1 Initial distance between gridpoints (m)
0.9 Timestep for numerical integration (s)
1 Mass of particles (kg)
1e+008 Spring stiffness axial springs stage 1 (N/m)
1e+007 Spring stiffness axial springs stage 1 (N/m)
8e+006 Spring stiffness shapesprings (N/m)
1.5e-009 Damping constant stage 1 (kg/s)
1.6e-008 Damping constant stage 2 (kg/s)
0.9 Reduction factor shapesprings (-)
500 Maximum mean of forces resultants on grid points stage 1 (N)
100 Maximum resultant of forces on any one grid point stage 2 (N)
400 Density of timber (kg/m3)
1.04e+010 Elastic modulus (N/m2)
0.05 Height of cross section (m)
0.05 Width of cross section (m)
4.108e+008 Characteristic bending strength (N/mm2)
0.5 Relaxation factor (-)

Results stage 1:

Accuracy indicators:

0.0533913m Mean difference of grid points with target surface
0.447681m Maximum difference at any one grid point
1.00521m Mean of distances between grid points
1.02326m Maximum distances between any two grid points
0.215672 Average unity check of grid points not on target shape
0.201 Average unity check of grid points on target shape

Shape forces (N):

i	j	Force
5	12	-186456
5	13	-21841
5	14	-126813
6	8	-452952
6	9	202525
6	10	-2.17612e+006
6	11	-792510
6	12	145432
6	13	203508
6	14	480561
6	15	-95780.4
7	7	-207703
7	8	626752
7	9	231290
7	10	518248
7	11	-148844
7	12	-39626.6
7	13	114817
7	14	233618
7	15	-177474
8	6	-3.65635e+006
8	7	565684
8	8	538953
8	9	315006
8	10	315897
8	11	545869
8	12	-175135
8	13	-134644
8	14	245346
8	15	-270232
9	6	-999328
9	7	520538
9	8	336657
9	9	335707
9	10	320991
9	11	480827
9	12	426477
9	13	113219
9	14	-1.03463e+006
10	6	-206401
10	7	510956
10	8	379987
10	9	369155

10	10	407483
10	11	540878
10	12	123826
10	13	315869
10	14	-218853
11	6	-213046
11	7	-172524
11	8	450012
11	9	321886
11	10	255926
11	11	70846.2
11	12	235013
11	13	585309
11	14	-64107.5
12	5	-477123
12	6	265160
12	7	-30988.6
12	8	-249861
12	9	314920
12	10	320873
12	11	398972
12	12	365215
12	13	378153
12	14	-50156.1
13	5	50476.5
13	6	128838
13	7	96427.5
13	8	-52989.7
13	9	209883
13	10	308555
13	11	683320
13	12	452530
13	13	1.2822e+006
13	14	-1.32131e+006
14	5	129698
14	6	237318
14	7	300407
14	8	144322
14	9	-1.58549e+006
14	10	61778.1
14	11	-155726
14	12	385228
14	13	-1.49724e+006
15	6	24384.7
15	7	-211747
15	8	247832
15	11	-2.22009e+006

Results stage 2:

Support reactions (N):

i	j	x	y	z
5	12	6020.09	-10457.7	-604.929
5	13	3762.56	-281.789	4787.78
5	14	5206.95	9315.04	-1753.47
6	8	1051.35	-34522.8	-22130
6	9	-5272.5	-64.2051	896.367
6	10	3130.55	163.753	1570.58
6	11	-1890.05	722.214	-8576.15
6	15	-7384.46	-4349.35	1535.4
7	7	6183.46	7010.25	7590.57
7	15	-951.043	-2345.76	1009.96
8	6	-29241.6	648.014	-16030.3
8	15	8319.12	-4831.35	2378.87
9	6	29350.3	-867.515	19389.9
9	14	-65518.5	-145.546	-31782.9
10	6	-6842.43	3238.36	-2369.31
10	14	2096.49	-6087.77	18468.3
11	6	15763.6	-2409.09	-2317.54
11	14	2950.28	5729.93	21533
12	5	-26225.5	6121.84	-9460.4
12	14	7375.34	2369.4	28633.8
13	5	2776	-2660.52	9829.6
13	14	48807.6	-2050.82	-45472.4
14	5	25256.5	85.4692	-1265.6
14	9	4636.37	2.45289	-13805.5
14	10	-10239.5	-1407.36	15591.1
14	12	-8682.65	1652.82	13238.8
14	13	-4802.18	48193.7	-54081.7
15	6	-5909.37	236.511	1752.38
15	7	-6604.44	-59.9209	4040.09
15	8	-704.851	-428.83	535.844
15	11	9.99728e+008	3.7987e+007	6.47651e+008

354.286N/mm2 Maximum allowable stress z

354.286N/mm2 Maximum allowable stress xy

Gridpoints where maximum allowable stress is exceeded (N/mm2):

i	j	sigmaz_i	sigmaxy_i	sigmaz_j	sigmaxy_j	Unitycheck

Remaining bending moments after relaxation (Nm):

i	j	Mz_i	Mz_j	Mxy_i	Mxy_j
5	12	-664.521	-530.756	124.297	-71.1876

5	13	-198.532	636.686	25.3626	306.542
6	8	-888.188	10.1612	355.836	-511.613
6	9	-321.778	1205.63	130.635	364.606
6	10	-948.891	246.213	55.661	-342.041
6	11	-914.927	-661.006	110.498	-610.881
6	12	11.6216	-107.804	-126.903	187.085
6	13	501.655	663.399	-160.112	321.089
6	14	906.278	787.39	-24.1689	-69.2458
7	7	-206.25	-356.904	370.131	-350.897
7	8	524.324	688.521	-42.9929	81.9342
7	9	417.772	940.747	-4.68601	43.284
7	10	471.744	514.616	20.1059	-8.105
7	11	310.354	-403.869	-36.6723	-411.076
7	12	305.658	-12.961	121.965	101.541
7	13	491.287	670.059	338.958	186.838
7	14	406.166	643.819	416.453	-201.649
8	6	-140.166	-1202.62	564.591	-211.688
8	7	512.294	630.489	-128.33	117.639
8	8	544.89	694.401	-148.218	81.7155
8	9	499.384	745.019	-128.281	-103.989
8	10	555.409	676.73	-117.483	120.571
8	11	483.658	-1.27241	-142.206	-158.943
8	12	251.402	274.849	-111.565	25.2422
8	13	-82.4454	390.24	-62.7319	-34.1618
8	14	-107.637	16.6582	35.61	-105.681
9	6	1024.96	-822.836	-218.26	-61.1421
9	7	983.157	686.308	-143.343	154.274
9	8	776.795	617.609	26.1473	51.1178
9	9	622.668	617.206	90.8428	-158.933
9	10	470.783	747.038	128.831	149.428
9	11	353.916	297.101	104.58	-30.7469
9	12	-75.2226	448.886	-70.457	18.1703
9	13	-456.668	437.204	-296.079	-190.316
10	6	-20.7212	-1119.82	497.799	-26.1577
10	7	240.923	569.668	127.04	170.237
10	8	458.637	632.75	-62.4658	29.4901
10	9	606.817	492.721	-125.338	-201.219
10	10	647.577	859.888	-100.672	150.409
10	11	607.329	285.365	-89.3875	-57.2532
10	12	561.286	631.239	-83.7622	85.4147
10	13	534.731	471.27	-106.195	-153.075
11	6	-263.106	-473.92	279.206	-83.1112
11	7	-161.432	296.501	285.359	149.081
11	8	246.266	523.166	53.6838	57.3933
11	9	496.207	244.325	-55.6114	-161.695
11	10	570.916	896.182	-52.1013	123.06
11	11	653.786	261.07	-24.0436	-87.8385
11	12	727.034	831.711	16.6908	97.1293
11	13	814.548	468.228	83.7083	-133.218
12	5	-815.99	-1029.44	324.655	-175.119

12	6	-159.704	247.584	-186.044	126.892
12	7	-17.7512	421.317	-140.469	-37.2375
12	8	290.852	204.891	-5.27335	56.9737
12	9	466.761	-167.986	3.98157	26.1823
12	10	549.072	945.111	-17.4338	93.7901
12	11	628.879	226.439	-9.09436	-94.6513
12	12	811.502	1055.06	21.8169	45.4798
12	13	858.463	418.043	63.2882	-106.082
13	5	492.462	-205.232	-291.673	58.4792
13	6	642.694	524.183	-311.951	70.7816
13	7	725.764	674.859	-182.474	-301.029
13	8	342.959	-218.144	48.3092	37.6942
13	9	369.414	-622.425	198.544	328.95
13	10	424.915	990.222	147.315	64.5504
13	11	444.907	280.548	137.569	-144.467
13	12	321.153	1145.61	113.552	-13.2977
13	13	380.045	383.016	168.159	-66.7977
14	5	738.562	230.452	40.5722	50.6188
14	6	732.074	666.406	141.09	-80.263
14	7	519.937	498.162	305.111	-354.327
14	8	-13.4251	-250.902	196.689	-45.8634
14	9	-1051.02	-1003.35	30.6604	677.874
14	10	-514.232	992.501	-135.552	63.5294
14	11	136.395	219.917	38.6133	-97.7864
14	12	-427.836	1361.6	-5.28667	-251.168

Grid point coordinates (m):

i	j	x	y	z
5	12	5.2055	10.4769	0.107106
5	13	4.99589	11.4477	0.232432
5	14	4.93008	12.4306	0.0546548
6	8	6.19526	6.61012	0.578153
6	9	6.17474	7.51767	1.00666
6	10	6.32396	8.50118	0.868665
6	11	6.31227	9.47197	0.617362
6	12	6.02341	10.4271	0.679658
6	13	5.82194	11.3996	0.793005
6	14	5.7711	12.3774	0.592098
6	15	5.7	13.2105	0.0444558
7	7	6.82889	5.82139	0.693304
7	8	6.82955	6.57356	1.35087
7	9	6.86667	7.49777	1.72886
7	10	6.92736	8.49325	1.6657
7	11	6.98159	9.44343	1.36074
7	12	6.84643	10.4271	1.24686
7	13	6.75921	11.4169	1.13927
7	14	6.76053	12.3264	0.724572
7	15	6.6901	13.0651	0.0546377
8	6	7.64584	5.2413	0.454013

8	7	7.62425	5.77873	1.29702
8	8	7.6367	6.54374	1.94076
8	9	7.68845	7.47598	2.29853
8	10	7.69406	8.47577	2.30689
8	11	7.75425	9.42411	1.99627
8	12	7.7422	10.3747	1.68708
8	13	7.74168	11.2764	1.25559
8	14	7.72802	12.0819	0.663856
8	15	7.67388	12.8813	0.0661857
9	6	8.56689	5.23823	0.852172
9	7	8.54392	5.78598	1.68817
9	8	8.56917	6.57551	2.30087
9	9	8.62195	7.50864	2.65613
9	10	8.60243	8.50621	2.72291
9	11	8.65222	9.4629	2.43595
9	12	8.68601	10.37	2.01569
9	13	8.72262	11.166	1.41098
9	14	8.69298	11.8204	0.654743
10	6	9.5585	5.33861	0.767063
10	7	9.5379	5.86214	1.61893
10	8	9.56896	6.59702	2.29632
10	9	9.61993	7.50005	2.72271
10	10	9.581	8.47861	2.92442
10	11	9.61253	9.45618	2.71691
10	12	9.61702	10.3968	2.37795
10	13	9.65347	11.1929	1.77411
10	14	9.63572	11.8348	1.00779
11	6	10.5483	5.20729	0.693829
11	7	10.52	5.87751	1.43555
11	8	10.5425	6.64719	2.07361
11	9	10.5939	7.55023	2.50019
11	10	10.5743	8.49852	2.81715
11	11	10.6124	9.49209	2.70986
11	12	10.6088	10.4652	2.47931
11	13	10.6433	11.2719	1.88892
11	14	10.6295	11.9281	1.13402
12	5	11.5616	4.21065	0.0704495
12	6	11.5118	4.94611	0.746544
12	7	11.5064	5.75861	1.32967
12	8	11.484	6.67142	1.73761
12	9	11.4866	7.62017	2.05382
12	10	11.5007	8.54026	2.44538
12	11	11.5609	9.53712	2.3941
12	12	11.5757	10.5242	2.23495
12	13	11.6046	11.31	1.61695
12	14	11.5954	11.9576	0.855145
13	5	12.5054	3.95781	0.296303
13	6	12.4879	4.77274	0.875021
13	7	12.4994	5.70618	1.23246
13	8	12.3694	6.69644	1.27388

13	9	12.2584	7.67914	1.41939
13	10	12.298	8.58285	1.84523
13	11	12.3726	9.57921	1.81004
13	12	12.3781	10.5648	1.64143
13	13	12.3775	11.3171	0.982569
13	14	12.3572	11.9361	0.19743
14	5	13.5004	3.83508	0.286451
14	6	13.4712	4.74547	0.698485
14	7	13.4012	5.7373	0.803228
14	8	13.1673	6.70049	0.671369
14	9	12.91	7.66679	0.659537
14	10	12.9591	8.57151	1.09699
14	11	13.0439	9.56966	1.06743
14	12	13.0814	10.562	0.932403
14	13	13.0222	11.271	0.219432
15	11	13.665	9.54929	0.282372

Initial grid point coordinates (m):

i	j	x	y	z
5	12	4.58991	10.5374	-1
5	13	4.58991	11.5374	-1
5	14	4.58991	12.5374	-1
6	8	5.58991	6.53743	-1
6	9	5.58991	7.53743	-1
6	10	5.58991	8.53743	-1
6	11	5.58991	9.53743	-1
6	12	5.58991	10.5374	-1
6	13	5.58991	11.5374	-1
6	14	5.58991	12.5374	-1
6	15	5.58991	13.5374	-1
7	7	6.58991	5.53743	-1
7	8	6.58991	6.53743	-1
7	9	6.58991	7.53743	-1
7	10	6.58991	8.53743	-1
7	11	6.58991	9.53743	-1
7	12	6.58991	10.5374	-1
7	13	6.58991	11.5374	-1
7	14	6.58991	12.5374	-1
7	15	6.58991	13.5374	-1
8	6	7.58991	4.53743	-1
8	7	7.58991	5.53743	-1
8	8	7.58991	6.53743	-1
8	9	7.58991	7.53743	-1
8	10	7.58991	8.53743	-1
8	11	7.58991	9.53743	-1
8	12	7.58991	10.5374	-1
8	13	7.58991	11.5374	-1
8	14	7.58991	12.5374	-1
8	15	7.58991	13.5374	-1

9	6	8.58991	4.53743	-1
9	7	8.58991	5.53743	-1
9	8	8.58991	6.53743	-1
9	9	8.58991	7.53743	-1
9	10	8.58991	8.53743	-1
9	11	8.58991	9.53743	-1
9	12	8.58991	10.5374	-1
9	13	8.58991	11.5374	-1
9	14	8.58991	12.5374	-1
10	6	9.58991	4.53743	-1
10	7	9.58991	5.53743	-1
10	8	9.58991	6.53743	-1
10	9	9.58991	7.53743	-1
10	10	9.58991	8.53743	-1
10	11	9.58991	9.53743	-1
10	12	9.58991	10.5374	-1
10	13	9.58991	11.5374	-1
10	14	9.58991	12.5374	-1
11	6	10.5899	4.53743	-1
11	7	10.5899	5.53743	-1
11	8	10.5899	6.53743	-1
11	9	10.5899	7.53743	-1
11	10	10.5899	8.53743	-1
11	11	10.5899	9.53743	-1
11	12	10.5899	10.5374	-1
11	13	10.5899	11.5374	-1
11	14	10.5899	12.5374	-1
12	5	11.5899	3.53743	-1
12	6	11.5899	4.53743	-1
12	7	11.5899	5.53743	-1
12	8	11.5899	6.53743	-1
12	9	11.5899	7.53743	-1
12	10	11.5899	8.53743	-1
12	11	11.5899	9.53743	-1
12	12	11.5899	10.5374	-1
12	13	11.5899	11.5374	-1
12	14	11.5899	12.5374	-1
13	5	12.5899	3.53743	-1
13	6	12.5899	4.53743	-1
13	7	12.5899	5.53743	-1
13	8	12.5899	6.53743	-1
13	9	12.5899	7.53743	-1
13	10	12.5899	8.53743	-1
13	11	12.5899	9.53743	-1
13	12	12.5899	10.5374	-1
13	13	12.5899	11.5374	-1
13	14	12.5899	12.5374	-1
14	5	13.5899	3.53743	-1
14	6	13.5899	4.53743	-1
14	7	13.5899	5.53743	-1

14	8	13.5899	6.53743	-1
14	9	13.5899	7.53743	-1
14	10	13.5899	8.53743	-1
14	11	13.5899	9.53743	-1
14	12	13.5899	10.5374	-1
14	13	13.5899	11.5374	-1
15	11	14.5899	9.53743	-1

References

[1] Barnes, MR 1999, *Form finding and analysis of tension structures by dynamic relaxation*

[2] Burkhardt, B, et al 1976, *Multihalle Mannheim*, Stuttgart: Institut für leichte flächentragwerke (IL13)

[3] Douthe, C, Baverel, O, Caron, JF 2006, *Form finding of a grid shell in composite materials*

[4] Hoefakker, JH, Blaauwendraad, J 2005, *Theory of Shells*, Lecture notes CT5143, Delft University of Technology, Delft

[5] Killian, A, Ochsendorf, J, *Particle-spring systems for structural form finding*

[6] Leuppi, J 2002, *Parametric design for the structural elements of timber rib shells,* Space Structures 5 volume 1, Thomas Telford, London

[7] Timoshenko, SP, Goodier, JN 1934, *Theory of Elasticity*, McGraw-Hill Book Company

[8] Toussaint, MH 2007, *A Design Tool for Timber Gridshells*, Msc thesis

[9] Vorst, HA van der, Wesseling, P, Wilders, P 1992, *Numerieke methoden voor differentiaalvergelijkingen,* Lecture notes WI3097, Delft University of Technology, Delft

[10] Welleman, JW 1992, *Combined spring element in Tilly,* TU Delft Report, Delft University of Technology, Delft